INTERNAL CYCLING IN AN URBAN DRINKING WATER RESERVOIR

Robyn R. Raftis

Submitted to the faculty of the University Graduate School
in partial fulfillment of the requirements
for the degree
Master of Science
in the Department of Earth Sciences,
Indiana University

October, 2007

Accepted by the Faculty of Indiana University, in partial fulfillment of the requirements for the degree of Master of Science.

Master's Thesis Committee

Gabriel M. Filippelli, Ph.D., Chair

Catherine Souch, Ph.D.

Lenore P. Tedesco, Ph.D.

ACKNOWLEDGMENTS

I would like to thank Gabe, Catherine, and Lenore for the loads of guidance they gave me on my journey through my Master's Thesis work. In addition, I am grateful to Abby Campbell, Cheryl Nazareth, Vince Hernly, Bob E. Hall, D. Lani Pascual, and Jennifer Latimer for their support and advice. Finally I would like to thank Veolia Water Indianapolis, LLC for providing the generous funding that supported the research conducted at Eagle Creek Reservoir.

Going after your dreams isn't always easy, but it sure feels good once you get there.

ABSTRACT

Robyn R. Raftis

INTERNAL CYCLING IN AN URBAN DRINKING WATER RESERVOIR

The focus of this study was to document phosphorus (P) and metal cycling in the Eagle Creek Reservoir (ECR), located in Indianapolis, central Indiana. Eagle Creek Reservoir serves the drinking water needs of over 80,000 residents. Within the last several years, algal blooms have created stress to the local treatment facility. The objective of this study was to examine how P cycling from oxygen deprived bottom sediments affects the algal bloom productivity. As such, cores were retrieved from different water depths (7 and 16 m) from portions of the reservoir where high surficial concentrations of organic matter and P were found to occur. The dried samples were analyzed for P, sulfur, iron, barium, cadmium, copper, lead, and zinc, using a strong acid digestion technique. The samples were also analyzed for iron-bound P (Fe-P), authigenic P (A-P), detrital P (D-P), organic P (O-P), reducible iron, and reducible manganese, using a sequential extraction technique.

The results from the study showed moisture contents ranged from 16 to 76% and organic matter contents ranged from 2 to 12 wt%. The dry bulk densities were determined to be between 0.27 and 1.68 g cm^3. The average percentages of P in ECS-1, as determined by the sequential extraction method, were as follows: Fe-P, 66.2%; A-P, 8.1%; D-P, 4.8%; and O-P, 20.9%. The average percentages of P in ECS-3, as

determined by the sequential extraction method, were as follows: Fe-P, 77.0%; A-P, 6.5%; D-P, 2.8%; and O-P, 16.7%.

To determine relationships between elements, correlations were calculated. When looking as the relationships between the P fractions and reducible Fe, differences were observed between the different water depths. There was less correlation between reducible Fe and Fe-P, and between O-P and Fe-P, in ECS-3, indicating that Fe-P is more efficiently dissolved and recycled in the deep portion of ECR. The study shows that the Fe-P flux, caused by the iron redox cycle, is persistent and will continue to influence algal bloom productivity in the deeper portions of ECR.

TABLE OF CONTENTS

1. INTRODUCTION

Worldwide, approximately 40,000 large dams (>15 m in height) and over 800,000 smaller dams, designed to store water for agriculture, industry, domestic use, hydroelectricity, and flood protection, are degrading at accelerated rates (Morris and Fan, 1998; Sharpley, 1999; EPA, 2004). Although water storage, hydroelectricity, and flood control measures are often important motivations for reservoir use, water quality generally degrades after time. Eutrophication, the rapid degradation of water quality marked by 1) increased productivity; 2) simplification of biotic communities; and 3) a decrease in the metabolism of organisms as a response to the imposed loading of nutrients, is often the process to blame, due in large part to nutrients from anthropogenic sources (Wetzel, 2001).

The nutrient phosphorus (P) is a major component in biological metabolism, yet there are relatively small amounts of P available in the hydrosphere in comparison to other vital nutrients such as carbon, hydrogen, nitrogen, oxygen, and sulfur; P is therefore often the limiting nutrient in fresh waters (Gardner and Eadie, 1980; Schlesinger, 1997; Sharpley, 1999). Phosphorus input from agricultural pesticide and fertilizer applications, urban runoff, and sediment pollution, strongly affect reservoir water quality, attributing P as the major non-point pollutant of concern in fresh waters (Schnoebelen *et al*., 1999). Given the right conditions, including elevated dissolved P levels, algal blooms degrade drinking water sources and potentially lead to the loss of beneficial aquatic life, after the decrease in dissolved oxygen (DO) levels associated with natural algal biomass degradation (Sharpley, 1999; Wetzel, 2001).

Figure 1 depicts the P cycle within a watershed that has both agricultural land uses and ongoing residential development. Greater than 90% of all P in fresh waters is present as phosphate, PO_4^{3-} adsorbed to inorganic and dead particulate organic matter, and as organic P and biotic cellular structure material. The majority of P supplied to a reservoir is rapidly deposited in the bottom sediments, resulting in sedimentary P concentrations as much as several orders of magnitude greater than that of the overlying waters (Wetzel, 2001).

At the sediment-water interface, P exchange between sediments and the overlying water column is a major component of the P cycle in lakes (Hutchinson, 1975). The stability of lake sediment P depends largely on the ability of the sediments to retain P. Phosphorus retention is controlled by the physical and chemical conditions of the overlying water column and pore waters, biotic redistribution of P, sediment geochemistry, and the local temperature and weather conditions. However, according to research completed by Nurnberg (1987), in undisturbed anoxic bottom waters, given sufficient time (2 weeks to 7 months), P may migrate from at least -20 cm sediment depth to overlying water. Song and Muller (1999) and Wetzel (2001) have also documented this affect.

The oxygen content at the sediment-water interface is a feature largely controlled by a) lake stability, b) the metabolism of bacteria, c) algae, fungi, and d) planktonic invertebrates that migrate to and live within the interface, and e) immobile benthic invertebrates, resulting in anoxia (DO < 1 mg/L as defined by Nurnberg, 1987) if left undisturbed by turbidity or thermal mixing. When oxygen is available, iron (Fe) is primarily insoluble Fe(III) hydroxides ($Fe(OH)_3$), marked by a brown, oxidized

microzone in experimentally defined laboratory lake sediment cores (Mortimer, 1942; Gorham, 1958; Wetzel, 2001). As oxygen levels approach zero, the reduction of these previously insoluble Fe compounds leads to the diffusion transport of dissolved Fe(II), until it once again is precipitated as Fe(III) at the oxic boundary (Figure 2).

As mentioned, oxygen regimes at the sediment-water interface are controlled by a number of factors. Organic matter decomposition plays a major role in redox geochemistry of lake sediments, and therefore the oxygen content (Wetzel, 2001). During the decomposition of organic matter, oxidants yielding the greatest free energy change per mole of organic carbon are used first; once this oxidant is depleted, oxidation will continue utilizing the next most efficient oxidant (Froelich *et al*., 1979). Within the oxic microzone, oxygen is the oxidant used to degrade organic matter, as long as it is available. Beneath this layer, MnO_2 and NO_3 reduction occur simultaneously, followed by iron oxide reduction, then $S0_4$, and finally methane fermentation dominates (Song and Muller, 1999).

Once anoxic conditions are achieved, P release from the sediments is controlled by chemical redox conditions, combined with biologic activity (Stumm and Morgan, 1996; Song and Muller, 1999). The potential for P recycling exists when the associated Fe(III) hydroxides are reduced (either by chemical or bacterial processes) and dissolve, thereby releasing adsorbed P (Hayes, 1964; Mortimer, 1971; Stumm and Morgan, 1996; Roden and Edmonds, 1997). The dissolved P may become redistributed within the water column by thermal mixing and/or turbulence caused by stormy or windy weather, or by the disruption of the microzone (flooding, dredging, etc.) (Boström *et al*., 1988; Roden, 1997; Schlesinger, 1997; Song and Muller, 1999; Wetzel, 2001). The amount of

dissolved P appears to be controlled by the precipitation of vivianite ($Fe_3(PO_4)^{2-}(H2O)_8$), a mineral formed during early diagenesis in lakes (Song and Muller, 1999).

Lake management and restoration efforts focusing on decreasing reservoir productivity and the resulting decreased basin volume have, thus far, concentrated on decreasing nutrient loading from watershed inputs by improving land management and by treating algal blooms (Holz, *et al*., 1997; Morris and Fan, 1998). Since the early 1900's, algal productivity is most commonly held in check by copper (Cu) algaecide treatments, either as preventative maintenance, or at bloom incidence; however, these treatments are strictly regulated by permits, and lake sediments are subsequently higher in Cu concentrations than in watersheds without treatment (Normandin, 1975). Thus the challenge facing reservoir P management should include targeting critical source areas of P, such as that retained in reservoir sediment, and defining potential threshold levels of sedimentary P.

1.1 Background and Other Studies

Sediment Phosphorus and Anoxia

Studies into the physical and chemical interactions at the sediment-water interface began in the early part of this century, forming a basic understanding of the role of redox chemistry on dissolution processes (Thienemann, 1928; Strøm, 1931; Mortimer, 1941; Hutchinson, 1957). Mortimer's studies on lakes in the 1940's were among the first to record an oxidized mud layer that caps redox processes until DO levels reach zero. Mortimer's 1941 study is now cited as initial proof for redox induced redissolution at the sediment-water interface (Wetzel, 2001). As evidence of the impact of internal reservoir P flux, Mortimer (1971) coupled his earlier findings to eutrophication and the role of P as

the limiting nutrient in lake productivity, which was quickly becoming an obvious problem facing water management professionals.

Work on nutrient loading/trophic level relationships by Vollenweider (1968) led to management efforts that dramatically decreased external P loads, yet algal productivity in lakes decreased only slightly or showed no change. The lack of noticeable improvements in reservoir water quality has since been attributed to internal P loads (Boström *et al*., 1988).

By 1984, Nurnberg created a method to calculate internal P loads from 1) estimates of P release rates from sediments, 2) the area of anoxia, and 3) a known period of time. The study was conducted using published data collected from 54 oxic lakes, 33 anoxic lakes, and 7 lakes that represented rapid changes in P concentrations in North America and Europe. Nurnberg (1985) concluded that internal P release significantly contributes to the P budget in lakes with anoxic hypolimnia, stating that surface water concentrations of P increased after fall turnover for Lake Magog, with as much as two-thirds available for biologic use.

After a four year study of Shagawa Lake, Minnesota, Larsen *et al*. (1981) found that at water depths below 6.5 m, the upper 10 cm of sediments could contribute significant amounts of P after anaerobic conditions began in late June until fall turnover. These studies indicate that P exchange at the sediment-water interface is much more complex than Fe redox chemistry as previously believed.

Roden and Edmonds (1997), and Caraco *et al*. (1998) attributed the role of biologic activity and the sulfur content of hypolimnetic waters to internal P redissolution processes based on laboratory core experiments. Roden *et al*. (1997) found that over time

inorganic phosphate (PO_4^{3-}) concentrations were 2-3.5 times higher in sediments amended with sulfates, which re-formed with the iron to create iron sulfide compounds. Caraco *et al*. (1998) found that water sulfate concentrations were an extremely important variable controlling P release from sediments because of the same Fe binding process. Boström *et al*. (1988) used sequential extraction of sedimentary P to demonstrate different retention mechanisms within lakes with differing physical properties, citing the significance of interactions between biological and abiotic processes.

Trace Metals

Trace metal concentrations were determined using the strong acid digestion technique and downcore trends were observed. Though Cu is a necessary trace element that is toxic at elevated levels, anthropogenic activities such as smelting, mining, sewage sludge, and algaecide activities increase amounts of biologically accessible Cu in the natural environment (Flemming and Trevors, 1989). Copper concentrations in surface waters without significant anthropogenic inputs are typically <20 μg/L (Moore, 1990).

Algaecide applications are used to control taste and odor compounds created by algal blooms that can be impossible to treat when groundwater mixing is not an option (Herring, 1976). Studies of sediments and fish tissue from common fish species in Lake George, Uganda reported 270 μg/g Cu in sediments and 189 μg/g Cu in liver tissue in 2 fish species, implying ecological health stresses in the lake (Lwanga *et al*., 2003).

Once mobilized as part of gasoline fuel exhaust, the toxic metal lead (Pb) stays in soils adjacent to roadways indefinitely. The use of leaded gasoline and lead-based house paints created major health problems in children (Filippelli *et al*., 2005). High child blood lead levels, which seriously affect IQ, were eventually attributed to lead in the

environment that was available to children most likely through hand-to-mouth contact. A subsequent ban on leaded gasoline and paint occurred in 1986. The Environmental Protection Agency (EPA) documented leaded gasoline use from 1967 to 1991 (Figure 3).

Data collected by Filippelli *et al*. (2005) indicated that residual soil lead remains and decreases in logarithmic concentrations away from a highly traveled roadway. The evidence suggests that lead concentrations in the sediments of the study site will reflect the impact of the leaded gasoline ban in the mid-eighties.

1.2 Objectives of This Study

No research exists on P geochemistry within Central Indiana lake or reservoir sediments. Little data exists on anthropogenic trace metal deposition in these sediments as well. Though physical lake properties are generally understood, detailed P and metal analyses are lacking, yet fundamental to long-term management of ECR. The primary goal of this research is to characterize P, sulfur (S), Fe, and trace metal biogeochemical cycling in Eagle Creek Reservoir (ECR) throughout the lifespan of the reservoir, to quantify and study P flux at the sediment-water interface as a function of seasonal hypolimnetic anoxia, and to historically chart iron-bound and organic-bound P accumulations within the reservoir.

To achieve this, elemental concentrations, accumulation rates, and detailed P geochemistry were used to determine the relative risk of P dissolution during anoxia, and the resulting flux from sediments. This data was then used to relate this flux to potential chemical binding processes between P, Fe, and S that occur in the hypolimnion during anoxia, as well as chart the history of anthropogenic trace metal deposition. Two sediment cores taken from different depths in the reservoir were studied. Though surficial

sediments were collected and analyzed for the ECR in 2002, accumulation rates and historical metal analysis have not been reported for ECR, and detailed P geochemistry has not been previously performed on ECR sediments. It is hoped that this study will be used as an aid in reservoir management, including those in other watersheds throughout the Midwest with similar characteristics.

2. STUDY AREA

The Eagle Creek Reservoir receives drainage from 419.58 km^2 of the Eagle Creek Watershed, has a surface area of 5.46 km^2, and was constructed in 1967 to provide flood control, eventually becoming a drinking water source for Indianapolis in 1976. Figure 4 shows the 2000 land use distribution for Eagle Creek Watershed. In 2000, 52% was agricultural, 4.3% was urban, and 9.3% was forest. Changes in land cover from 1985 to 2000 show decreases in agricultural land cover and increases in grassland, high density, and low density land cover, which includes urbanized land (Tedesco *et al*., 2003).

The 12th largest municipal park in the U.S., Eagle Creek Park, borders the reservoir (over 15 km^2), offering recreational activities such as swimming, boating, fishing, and sporting events. The reservoir currently serves the drinking water needs for over 80,000 residents of Indianapolis (Tedesco *et al*., 2003). Its holding capacity is over 29,526 km^3, and the maximum depth ranges from about 12 to 16 m, with the deepest area located in the southern portion of the reservoir. The deepest regions of the reservoir represent the old Eagle Creek channel, as demonstrated by the bathymetry contours in Figure 5 (Tedesco *et al*., 2003). The total bottom surface area of the reservoir is estimated to be 5.01 km^2.

Eagle Creek Reservoir is located in the White River Basin, which experiences a humid continental climate, and is characterized by large annual temperature ranges and well-defined summer and winter seasons. Precipitation is characterized by long duration and mild intensity storms in cooler months, and short duration, higher intensity storms in the late spring and summer months (National Weather Service, 1990) (Table 1). The ECR is fed by 10 subwatersheds within the Eagle Creek Watershed, which is located on the

northwestern edge of Indianapolis. The major contributing streams are Fishback Creek, School Branch, and Eagle Creek. The bedrock of the Eagle Creek watershed is Devonian-aged black shale, limestone, and dolomite (Gray *et al*., 1987). Surficial deposits are Wisconsin age till, loam, and silty loam (Gray *et al*., 1989); defined physiographically as the Tipton Till Plain (Schneider, 1966).

In early spring, 2003, water temperatures were 14^{o}C throughout, thus there was relatively little resistance to mixing by wind energy. As spring continued in ECR in 2003, water temperatures became stratified at depths greater than 4 m, and stayed stratified until early October. The ECR DO concentrations for spring 2003 were 12 mg/L throughout. During summer stratification, surface water DO concentrations were between 8 and 10 mg/L, while at depths below 6 m DO was often zero. Dissolved oxygen became consistent again throughout the water column, in early October, following fall turnover.

The specific conductance of ECR waters stays consistently above 300 mV until summer stratification, at which time values as low as -50 mV are found in the hypolimnia up to 3 m water depth (Tedesco *et al*., 2003). Values of <-50 mV are known to be associated with dissolved P reflux in studies conducted at the sediment water interface (Mortimer, 1942; Wetzel, 2001)

The Eagle Creek Reservoir (ECR) has been periodically treated with a chemical algaecide to control algal blooms most commonly caused by the blue green algae *Pseudanabaena,* since 2000 (Table 2) (Tedesco *et al*., 2003). The chemical used in ECR is a copper-ethanolamine complex (Cutrine-plus; CP), a chelated Cu algaecide that is applied to a reservoir surface from boats with spray equipment (Tedesco *et al*., 2003).

Tedesco *et al*. (2003) led a pilot study that included geochemical analysis on the sediment P and metal geochemistry of the reservoir bottom sediments in ECR to define compositions and distributions during the last 5-10 years and shed light on the algal bloom problem. Grain size and organic matter concentrations were measured, and barium (Ba), cadmium (Cd), Cu, Fe, Pb, and Zinc (Zn) concentrations were determined (Table 3). Phosphorus concentrations were generally high (0.3-4.5 mg/g) in relation to background soil levels (0.5-2 mg/g). Concentrations of sediment Cu were high compared to background levels, ranging from 24 μg/g to 137 μg/g (Tedesco *et al*., 2003). The increased concentrations are related to copper algaecide applications, as the highest concentrations are found in the middle third and the south portion of the reservoir (average 71 μg/g Cu), directly above and south (down-flow) of routine algaecide applications.

In 1983, the United States Geological Survey (USGS) collected stream bed data for Eagle Creek. Streambed sediments upstream of ECR averaged 19 μg/g (Wangsness, 1983).

3. METHODS

Two cores that are believed to represent two different hypolimnetic oxygen regimes within ECR, based on physical and surficial data, were recovered in November of 2003, using a Mooring Systems, Inc. gravity corer. The locations were chosen by two factors, high concentrations of organic matter and total P recorded during initial surficial geochemical study, and water depth (Figure 5). High organic matter locations were selected because the rate of biological productivity is most likely higher in these regions, thus increasing the anoxia potential. Locations in which higher surfical P concentrations corresponded to high organic matter contents were chosen with the same assumption that greater biological productivity occurs at these sites. By choosing sites with similar organic matter contents and surficial P concentrations, the affects of anoxia are monitored at sites with different water depths.

A total of four 2-inch diameter cores were taken using a gravity corer system. Core liners were utilized to protect sediments from contamination. Core compaction was measured as the difference in core penetration and core recovery. The core extracted from the 7 m water depth was 55 cm in length, with 28% compaction; the core extracted from the 16 m water depth was 109 cm in length, with 34% compaction. The cores were kept upright during travel from the reservoir to the laboratory and refrigerated at 10^{o}C, then split in half lengthwise with a circular saw within 3 hours of retrieval. The stratigraphy and sedimentology of the cores were photographed and described (in terms of composition, presence of root/stem/leaf fibers, color, grain size and shape), and sediments were sampled for solid-phase analyses. Wet and dry bulk density (DBD) samples were measured from 1 cm intervals using a plastic 5 cc syringe and volumes

were recorded, then the samples were weighed wet, put in an oven at 105^{o}C overnight to dry, put into desiccators to cool, and then re-weighed before being transferred into scintillation vials for storage. Additional sub-samples were taken at 1 cm intervals, weighed, and frozen. After 24 hours the frozen samples were placed in a Virtis Benchtop freeze dryer for 24 hours, and reweighed. Freeze dried samples were required for sequential extraction and grain size analyses. The samples were then transferred to clean 20 mL scintillation vials.

Percent moisture content was calculated by subtracting the sample dry weight from wet weight, dividing by the wet weight, and then multiplying by 100. Loss on ignition (LOI) and grain size analyses were completed in order to distinguish lake sediments from pre-reservoir sediments and to correlate with other lake data. The LOI was used to determine the organic matter content of the sediments. An accurately weighed sample mass was placed in acid cleaned, dry, pre-weighed porcelain crucibles, ashed in a muffle furnace at 550^{o}C for approximately 2.5 hours, cooled in a dessicator, and reweighed. Grain size analysis was conducted on the Malvern Instruments Mastersizer 2000 after a 30% hydrogen peroxide treatment to remove organics. The average percentages of sand, silt, and clay were obtained from three replicates. Recording magnetic susceptibility from sediments determined the magnetizability of sediments, indicating a difference in source material. Magnetic susceptibility was performed on 5 cm intervals of the core from the deep portion of the reservoir (ECS-3) using a Bartington MS_2C Core Logging Sensor. Average annual sedimentation rates, necessary for P and metal accumulation calculations, were determined by first correcting core lengths for

compaction effects, then using interpreted reservoir sediment lengths, divided by the life span of the reservoir (37 years).

Total Phosphorus, Sulfur, and Metals

Two of the cores collected from ECR were used to characterize interactions within the hypoliminion of two different water depths, based on their location and good core recovery. The samples underwent a strong-acid digestion, releasing into solution total P and all but the refractory fraction of trace metals, which are biologically accessible. The ashed sample residues were placed in new 50 mL polypropylene centrifuge tubes, bathed in 25 mL 2N HCl, and shaken for approximately 24 hours, then centrifuged. Total P was analyzed to compare to surficial distributions previously recorded within the reservoir, and compare to sequential P extraction data. Trace metals selected for the study were Ba, Cd, Cu, Fe, Pb, and Zn, to trace changes in concentrations within the sediments and to better qualify the age of sediments. Sulfur was analyzed as it is an important contributor in the iron cycle in the hypolimnia. Iron contents, both oxidized and reduced concentrations, were studied to relate anoxic sediment-water interface iron chemistry to P flux.

Geochemical analyses were performed on a Leeman Labs PS950 Sequential Inductively Coupled Plasma Atomic Emission Spectrometer (ICP-AES) fitted with a CETAC AT5000+ ultrasonic nebulization system for improved detection limits. For this analysis, approximately 0.6 mL extractant from the digestion procedure was diluted 1:11 with acidified Milli-Q water. The results (in ppm solution) were back-calculated to solid concentrations (also in ppm) taking into account sample dilution, extractant volume, and initial sample mass.

Sequential Phosphorus Extraction

In order to investigate the different forms of P within the top portion of sediments, sequential extraction experiments such as the modified SEDEX method (Ruttenberg, 1992; Anderson and Delaney, 2000) allow sedimentary P components to be defined experimentally (Table 4). The first fraction of P isolated, oxide-reducible and adsorbed P (Fe-P), represents reactive iron and manganese minerals with adsorbed or coprecipitated P, including some clay minerals. This fraction of P in sediments has the greatest impact on the redistribution of bioavailable P upon the onset of low oxygen conditions. The second fraction, authigenic and biogenic P (A-P), represents sources of P that are related to P that forms *in situ*, and that which is derived from the physiological processes of organisms. This includes the roughly 90% of inorganic particulate P and organic particulate P found in inorganic cellular parts. P related to $CaCO_3$ is included in this fraction. The third P fraction studied was detrital mineral P from igneous and metamorphic sources (D-P). Last is P associated with organic matter, pertaining to compounds containing carbon (O-P).

The modified sequential extraction method chemically isolated ECR P into four sedimentary components, depending on the dissolution characteristics of the components and carefully optimized reagent strengths, acid strengths, reaction order, and reaction times. This process also releases reducible Fe and Mn, which both behave similarly with regards to P. Approximately 100 mg freeze dried sample was ground, weighed, and placed into new 15 mL polypropylene centrifuge tubes, including replicates and Standard Reference Material (SRM) 1646a, estuarine sediment (National Institute of Standards and Technology). Each reaction utilized an orbital shaker to keep samples suspended

achieving optimal dissolution. At the end of each reaction, the samples were centrifuged at 4500 rpm for 10 minutes, and then the supernatants were decanted from the centrifuged samples into acid cleaned polyethylene collection bottles.

When an extraction step required multiple treatments, the supernatants were combined into one collection bottle. Care was taken throughout the procedure to ensure that contamination by laboratory detergents did not occur by restricting use of such detergents on the counter tops and sample containers; acid cleaning was used instead (1N HCl at 60^{o}C for at least 24 hours). Milli-Q water was used for reagent preparation and water washes, as well as final rinsing of collection bottles and analysis containers.

A Shimadzu UV-2401PC scanning spectrophotometer was used to determine P concentrations for all steps other than the Fe-P, using the standard ascorbic acid molybdate blue technique (Strickland and Parsons, 1972) for color development. The presence of the citrate-dithionite buffer used for Fe-P interferes with the reduction of the molybdate-P complex, and therefore this P was determined using ICP-AES. Average standard deviations and typical detection limits are presented in Table 6.

The accumulation rates of O-P and Fe-P were calculated by multiplying the dry bulk density (g cm^{-3}) and element concentration (μg/g) of each depth interval by the sedimentation rate (cm^2/yr) and bottom surface area (cm^2).

4. RESULTS

Tables 5 and 6 present the physical and geochemical data collected on the two cores selected for analysis. Geochemical analyses of P, S, Ba, Cd, Cu, Fe, Pb, and Zn were performed. Detailed P sequential extractions of the upper top 38 cm of sediment samples documented changes in P fractions.

4.1. Sedimentology

The Munsell colors and textures of the ECR cores are generally uniform for the deepest portions of the cores (5Y 3/1) and the top ~50 cm of each core (alternating laminae of 5Y 3/2 and 5Y 2.5/1). Figure 6 is the core description and photograph for ECS-1 (7 m water depth). At the base of the core poorly sorted sandy mud with roots was present. At 48 cm depth, a sharp contact of black, organic rich, fine-grained sediments was noted. The contact was followed by gray, layered mud. Organic rich laminae (1 mm) were present from 48 to 4 cm. The sediments were disturbed and very fluffy from 4 cm to the surface.

Figure 7 is the core description and photograph for ECS-3 (16 m water depth). At the base of the core is poorly sorted sandy mud with roots, followed by well-sorted brown clay (2.5Y 4/3-2.5Y 4/4), with some organic layers up to 2 cm thick, to 65 cm. A sharp, organic rich contact was noted at 65 cm, followed by gray, layered mud. The same organic rich laminae present in ECS-1 were present to about 3 cm, with the surface sediments disturbed and fluffy.

Moisture contents range from 16-76% in the core samples (Table 5). In general, both cores display an increase in sediment moisture content after the organic-rich contact. Before the contact, sediments in ECS-1 have low moisture contents (around 3.3%),

followed by an increase in moisture contents (around 9.4%). The sediments in the bottom 9 cm of the core display similar moisture contents to the sediments in ECS-1 that were below 49 cm to 55 cm. The brown sediments from 100 cm to 66 cm have a moisture contents average of 4.6 wt%. After the contact at 65 cm, the sediments are again similar to the upper portion of sediments in ECS-1 (Figure 6 and 7).

Dry bulk density ranges from 0.39 to 1.5 g cm^{-3} for both cores (Table 5). The lower most sediments range from about 1.2 to 1.7 g cm^{-3}, with an average of 1.2 g cm^{-3}. Above the organic-rich contact, sediment dry bulk density decreases to 0.79 to 0.39 g cm^{-3}, averaging 0.52 g cm^{-3} (Figures 6 and 7). The sediment dry bulk density between the depths of 100 cm and 66 cm range from 1.0 to1.5 g $cm^{-3,}$ averaging 1.4 g cm^{-3}.

The magnetic susceptibility (MS) of ECS-3 is highest in the sediments characterized by poorly sorted mud with roots, averaging 59 cm g^{-1} s^{-1} (CGS), then sharply dropping in the sediments at about 97 cm depth to an average of 25 CGS. This trend slowly decreases to an average of 12 CGS from 65 cm to the surface sediments (Figure 7). Organic matter contents range from about 1.9 wt% to 12 wt% for both cores. Sediments from 49 to 55 cm in ECS-1 and 109 to 100 cm in ECS-3 have an average organic matter content of 3.3 wt%. Sediments from ECS-3 in the core section from 101 cm to 66 cm have an average organic matter content of 4.6 wt%. The sediments above the contact average 9.4 wt% organic matter content (Figures 6 and 7).

Grain size analysis was performed on samples chosen above and below the sharp organic contact noted at 48 cm in ECS-1 and 65 cm in ECS-3. Figure 8 shows the grain size distribution of sediment samples collected from the cores at different depth intervals.

Sediments collected from above the contact in both cores are about 43% clay and 57% silt. Sediments collected from the 66 to 100 cm depths in ECS-3 display about 40% clay, 50% silt, and 10% sand. The grain size distributions of the sediments from the bottom portions of the cores are generally 20% clay, 40% silt, and 40% sand.

4.2 Major Element Chemistry and Metal Geochemistry

Total P concentrations range from about 0.7 to 3.3 mg/g (Table 6); (Figure 8). Sediments below the contact layer in both cores (49 cm in ECS-1 and 65 cm in ECS-3) average 1 mg/g P, and sediments above the contact average 2 mg/g P. In general, ECS-3 sediments above the contact layer displayed higher average P concentrations than those of ECS-1.

Iron concentrations range from about 2 to 14 wt% with an average of about 6 wt% (Table 6) (Figure 8). ECS-1 lower most sediment Fe concentrations average 3 wt%, and sediments above the organic-rich contact at 49 cm Fe contents average 5 wt%. ECS-3 lower most sediments average 2.6 wt%, sediments between 65 and 100 cm depth average 4.6 wt%, and sediments above the contact at 69 cm average 7 wt%.

Sulfur (S) concentrations range from about 0.08 to 0.84 wt% with an average of about 0.33 wt% (Table 6) (Figure 8). ECS-1 sediment S concentrations in the lower most portion of the core average 0.11 wt%, and sediment S contents above the 49 cm contact layer average 0.27 wt%. In ECS-3, the lower most sediment portion of sediments average 0.18 wt%; sediments between 65 and 100 cm depth average 0.26 wt%; and sediments overlying the contact at 69 cm average 0.38 wt% S.

Trace Metals

ECR sediment trace metal concentrations are summarized in Table 6 and are graphically represented in Figure 9. Reducible Fe and Mn will be discussed later in this section.

Copper concentrations range from about 7 to 47 μg/g in ECS-1, and from about 10 to 67 μg/g in ECS-3 (Table 6). ECS-1 and ECS-3 lower most sediment portions (48 to 55 cm in ECS-1 and 100 to 109 cm in ECS-3) Cu concentrations average 15 μg/g and 30 μg/g, respectively. The ECS-3 Cu concentrations of the sediments between 65 and 100 cm depth average 45 μg/g. ECS-1 and 3 sediment Cu concentrations above the contact average 21 μg/g and 28 μg/g, respectively. Based on average sediment Cu concentrations before algaecide applications, from the contact at 49 cm to 10 cm in ECS-1 (17.1 μg/g), and from the contact at 69 cm to 15 cm (22.9 μg/g), background Cu concentrations for ECR sediments above the organic-rich contact average 20 μg/g.

Cadmium concentrations range from about 7 to 13 μg/g (Table 6). The Cd concentrations of the lower most sediments for ECS-1 and ECS-3 average 8.5 μg/g and 9.37 μg/g, respectively. The ECS-3 Cd concentrations of the sediments between 65 and 100 cm depth average 11 μg/g. ECS-1 and 3 Cd concentrations average 12 μg/g above the organic rich contact at 49 and 65 cm, respectively.

Barium (Ba) concentrations range from about 3 to 276 μg/g (Table 6). Sediment Ba concentrations for the lower most sediments in ECS-1 average 50 μg/g and sediment concentrations above the contact at 49 cm average 153 μg/g. ECS-3 sediments from 100 to 109 cm showed Ba concentrations average 49 μg/g, the sediments between 65 and 100

cm depth average 77 μg/g, and sediment concentrations average 156 μg/g above the organic-rich contact layer.

Lead concentrations range from about 7 to 70 μg/g (Table 6). ECS-1 and 3 sediment Pb concentrations in the lower most portions of core average 21.3 μg/g and 20.5 μg/g, respectively. The ECS-3 Pb concentrations of the sediments between 65 and 100 cm depth average 31 μg/g. ECS-1 and 3 sediment Pb concentrations from the sediments above the contact layer average 46 μg/g and 48 μg/g, respectvely.

Zinc exhibits the highest concentrations of all trace metals in both cores, ranging from about 66 to 278 μg/g (Table 6). ECS-1 and 3 pre-reservoir sediment Zn concentrations average 75 μg/g and 102 μg/g, respectively. The ECS-3 Zn concentrations of the sediments between 65 and 100 cm depth average 165 μg/g. ECS-1 and 3 reservoir sediment Zn concentrations average 180 μg/g.

The determinations of reducible Fe and Mn were found by analyzing the P sequential extraction samples, which was only performed on the top most reactive sediments (upper 38 cm). ECS-1 reducible Fe concentrations range from about 0.8 to 1.8 wt%; ECS-3 reducible Fe concentrations range from about 0.5 to 1.3 wt% (Table 8). ECS-1 reducible Mn concentrations range from about 565 μg/g to 1238 μg/g; ECS-3 reducible Mn concentrations range from about 806 to 1265 μg/g.

4.3 Detailed Phosphorus Geochemistry

The top 38 cm of the core sediments were analyzed at 1 cm intervals for sequential P (Table 7). Fe-P concentrations range from about 0.2 to 2 mg/g, and average 0.8 mg/g for ECS-1 and 1.3 mg/g for ECS-1. A-P concentrations range from about 0.06 to 0.1 mg/g, and average 0.1 mg/g for both ECS-1 and 3. D-P concentrations range from

about 0.03 to 0.09 mg/g, and average 0.05 for both cores. O-P concentrations range from 0.2 to 0.4 mg/g, and average 0.2 for ECS-1 and 0.3 for ECS-3.

The concentrations were converted into percentages based on the total concentrations of P. ECS-1 had a Fe-P concentration range of 55-74%, with an average of 66%. ECS-3 had a Fe-P concentration range of 68-78%, and an average of 74%. A-P concentrations range from 4-10% in ECS-1 and average 8% in ECS-1, and range from 5-8% in ECS-3 and average 7%. D-P concentrations range from 3-11% in ECS-1 and average 5%, and range from 2-5% in ECS-3 and average 3%. O-P concentrations range from 16-25% in ECS-1 and average 21%, and range from 13-20% in ECS-3 and average 17%.

Accumulation rates were calculated for the O-P and Fe-P with the available geochemical data (elemental concentration, dry bulk density, and bottom surface area of ECR). The average accumulation rate for Fe-P in the Eagle Creek Reservoir is 49 metric tons per year (mt/yr). The average accumulation rate for the organic fraction of P is 12 mt/yr.

5. DISCUSSION

The sedimentology of ECR cores will be discussed, followed by a discussion of the depositional history of ECR sediments as recorded in the geochemical data for the study cores. Finally, the P fractions determined by sequential extraction will be discussed.

5.1. Sedimentology

After examination of the core sediments, 3 sediments types with distinctly different textures and compositions (Figures 6 and 7). Identifying the point of change between sediment types is necessary for recognizing the point at which the reservoir setting dominated the area, characterized by a smaller grain size and higher organic matter contents relative to soils that would have been present before the construction of ECR.

The first sediment type to be discussed is that in the lower most portions of the cores, 49 to 55 cm in ECS-1 and 100 to 109 cm in ECS-3. In these depth intervals the cores contain plant roots, 1 to 2% pebbles, and 30% poorly sorted sand in the deeper portions. These characteristics are similar to soils in the area, the Miami-Crosby soil association where the sediment distributions are 27 to 35% clay, 15 to 40% sand, and 0 to 10% rock fragments. Therefore these sediments are believed to be from before the reservoir was in place.

The evidence of a dark, fine-grained contact at the termination of these sediments also indicates a change in depositional environments; therefore, it is believed that this point in the cores marks the beginning of a stable reservoir environment. Evidence of an unstable and evolving environment is noted in the shift in sediment in the first 2 to 6 cm

of sediments after the black contact, and in the sediments between 99 and 65 cm in ECS-3.

The grain size distribution of these sediments is unlike that of the underlying and overlying sediments, but they are more similar to the underlying, soil-like sediments (28 to 38% clay, 43 to 58% silt, and 3 to 30% sand). The sediments at 65 to 99 cm in ECS-3 could have originated in a number of different ways, and a few hypotheses will be presented; however, although interesting from a historical perspective, the important idea to note is that the sediments represent a shift from one relatively constant state (soils) to another (lake sediments). The sediments seem to likely represent the initial phases of the reservoir, when the soils present would be initially uplifted and resorted in the calm regions of the early reservoir in the south end.

The brown sediments may also represent infill material used either in the construction of the dam itself, or the construction of the marina directly east of the core location (Figure 4). The last possibility, provided through personal communication with long-time Indianapolis resident and geologist, James Nowacki, is the creation of the rowing aisles in the north basin of the reservoir, which were constructed shortly after the initial flooding of the watershed. Aerial photographs and/or site descriptions of Eagle Creek, immediately before the inundation of the flood plain, were not available to verify the environment of deposition for these sediments.

Historical aerial photography taken in 1956 shows the site as it was before the presence of the reservoir, the Eagle Creek Flood Plain, adjacent to Eagle Creek; the area was then predominantly used for agricultural purposes. The sediments distinguished by sandy mud with roots in the lower most portions of the cores, 49 to 55 cm in ECS-1, and

100 to 109 cm in ECS-3, is believed to be from the flood plain and before the creation of the ECR. Because of the different depositional environments, the sediments displayed a stark distinction that was used to distinguish and recreate the history of the area that is now a reservoir. The sediments characterized by reservoir deposits (Figure 6 and 7) showed fine-grained clay with 1 mm laminae alternating in organic matter content and black color, with a grain size distribution of 38 to 45% clay, 55 to 63% silt, and less than 1% sand.

Also depicted in Figures 6 and 7 are the moisture contents, dry bulk densities, and organic matter content, which also display shifts due to depositional differences between soils before flooding and fine-grained reservoir sediments after. Magnetic susceptibility was measured on ECS-3 only due to instrument availability. Based on these physical and sedimentalogical differences, the sediments were divided at the organic rich layer between a soil unit, followed by a reservoir unit. The sediment unit between the two in ECS-3 is ignored for the purposes of this report. It is also important to note that the disturbance of the top 4 cm or so of each core also disallows detailed evaluation of elemental concentrations. This is due to the type of coring method used.

Moisture contents rose sharply, from less than 20% at about 50 cm depth in ECS-1, and then stabilized at about 48 cm, to 60% in surface sediments. The sediment DBD is negatively correlated to moisture contents in the ECS-1, decreasing from around 1.4 g cm^{-3} in the sediments classified as soil to 0.5 g cm^{-3} in reservoir sediments. The DBD values from 5 cm depth to surface increase from 0.4 to 6.5 g cm-3. The shift to higher bulk densities in the top 6 cm of ECS-1 is attributed to sampling error because the sediments were over 50% moisture and therefore more difficult to work with. The same

trend was not noted in ECS-3 as well (Figure 6). In general, moisture contents and dry bulk densities were the same in ECS-3.

The average DBD of soil sediments (soils average 1.58 g cm^{-3}) (Table 5) agrees with Miami-Crosby soil DBD average values, 1.5 g cm^{-3} (NRCS, 2005). The magnetic susceptibility (MS) recorded from ECS-3 sediments is further evidence of the division of the two basic sediment signatures noted in the cores (Figure 7). The MS values for both soil and reservoir sediments agree with values known to occur in similar sediments types (Hanesch and Scholger, 2005). The DBD and moisture contents change with sediment type in both cores, at 48 cm in ECS-1 and 69 cm in ECS-3. These profiles for DBD and moisture content are expected for reservoir sediments.

Organic matter content in both cores corresponds well to moisture content. The organic matter content of the reservoir sediments (9 wt%) is comparable to other mid-western lakes, which range from 11 wt% in Lake Shagawa, Minnesota (Larsen *et al*., 1981) to 16 wt% in Canadohta Lake, northern Pennsylvania (Roden *et al*., 1997).

The organic matter content profiles are generally identical in both cores (Figure 6 and 7). Values average about 3.5 wt% in soil sediments and about 10 wt% for lake sediments. The organic matter content of the pre-reservoir sediments are slightly higher than those of Marion County soils adjacent the reservoir (1.2 wt% NRCS, 2005). Organic matter content in reservoir sediments is greater than that of the underlying soil, as expected, because the basin acts as a trap for organic particles, in contrast to the flood plain environment that existed before the construction of the reservoir where oxidation and weathering were factors of organic matter content.

The downcore profiles of the reservoir sediments are similar to those reported in other organic-rich sediments. Organic matter contents decrease downcore as a result of decomposition (Song and Muller, 1999). Other geochemical profiles corresponding to that of organic matter and decomposition will be discussed later.

The physical features and steady values that are recorded downcore for DBD, moisture, organic matter, and grain size in both cores, before and after the organic-rich contact, are indicators that the assumption that sedimentation has been mostly consistent through time is likely valid, enough so that sedimentation rates may be used to calculate P accumulation rates in ECR. Consequently, sediment age, sedimentation rates, and accumulation rates of P and metals are acquired based upon these distinctions in sedimentology.

Using the proposed flood boundaries from each core, assuming constant sedimentation, and correcting for compaction, average sedimentation rate is 1.7 cm/yr for ECS-1 and 2.4 cm/yr for ECS-3.

The calculated sedimentation rates for each of the ECR cores are comparable, but the rate is lower in ECS-1. Both sites are located near or in the old channel of Eagle Creek and the difference in sedimentation rates may be partly explained by the undercurrent in this channel, seen as bathymetric lows in the reservoir (Figure 4). The slightly slower sedimentation rate at ECS-1 is attributed to a stronger current energy and the subsequent erosion that would take place in the old channel during times of high current flow. While the higher rate in ECS-3 is partly due to the slope of the deeper basin and decreased energy.

5.2 Major Element and Metal Geochemistry

Based on the organic-rich contact, the elemental geochemistry of the two sediment units was also different for many elements selected for analysis. The sediments between 65 and 100 cm in ECS-3 will therefore not be discussed in the following sections. In general, the pre-reservoir sediments have concentrations as much as 3 times lower in total P and metals than reservoir sediments (Figures 8 and 9). Some of the peaks reported for metal concentrations downcore correspond to historical additions to the reservoir.

Phosphorus, Iron, and Sulfur

The depositional patterns of P are much more constant in the soil unit, ranging from 0.5 mg/g to l.2 mg/g in ECS-3, than in the reservoir unit, which ranged from a minimum in ECS-1 of 1.2 mg/g, to a maximum of 3.5 mg/g in ECS-3. The variability noted in the reservoir unit is opposite to the consistency noted in physical properties such as moisture content, grain size, and DBD. Phosphorus is concentrated in reservoir sediments than in the soil.

Between the reservoir sediments in each core, the sediments are similar up to about 25 to 40 cm, and then the concentrations jump in ESC-3 for the following 20 cm before both cores contain about 2.2 mg/g, then sediment P concentrations increase again in ECS-3. The higher variability in ECS-3 P may suggest that the area has experienced periods of high reactivity. Mineralization of organic matter causes the P to be constant in the deeper portions of the cores, where P is no longer reactive (Song and Muller, 1999).

The total P concentrations of the reservoir sediments are similar to values found in surficial ECR sediments, and are also comparable to concentrations found in Geist

Reservoir (GR) and Morse Reservoir (MR), also located in central Indiana, near Indianpolis (Table 2). The reservoir sediment total P concentrations also agree with those found in Shagawa Lake, Minnesota (Table 8).

Iron increases in reservoir sediments but not as sharply, following the contact. Iron is similar in each core and is shown in higher concentrations in reservoir sediments most likely due to fine-grained sediment accumulation. Iron concentrations in ECR reservoir sediments are similar to the surficial study data and for the surficial study data collected for GR and MR.

The S concentrations in the soil unit of ECS-1 are lower, less than 0.2 wt%, but S concentrations drop in ECS-3 after the contact to slightly lower than ECS-1. However, for the most part the trends are similar until about 17 cm in ECS-1 and 23 cm in ECS-3, when concentrations jump in ECS-3 to about 0.5 wt%. Sulfur concentrations agree with those determined for ECR, GR, and MR surficial sediments (Table 3).

Elemental correlations, as Pearson's R, are reported in Table 9. Graphical representations of the relationships between P, Fe, S, and organic matter (OM) are found in Figure 9. Studying the different relationships between cores reveals evidence for the prevalence of anoxia in the deep basin (ECS-3).

The correlation between total P and OM is much greater in ECS-3 (R=0.77), than in ECS-1 (R=0.33) (Figure 10a). This data suggests that organic matter decomposition is greater in the deeper portion where anoxic decomposition is believed to occur for longer periods throughout the year. In other words, anoxia due to organic matter decomposition is more likely a factor in the south portion of the reservoir where deeper waters and high organic matter contents dominate. It may also mean that there are slightly more samples

from the anoxic layer of the ECS-3 core; however, the correlation in ECS-3 is strong enough to indicate that the deposition of total P is directly correlated to that of OM, and only weakly so in ECS-1.

Organic matter is not correlated to S, or total Fe in either core (Table 9) (Figure 10b and 10c). It is not expected that a relationship would necessarily exist between OM and total Fe due to the contrasting sedimentary sources of these two elements. A slight correlation exists between S and OM, indicating that sulfate reduction may be occurring in the anoxic layer of sediments in ECR, but this could also be a factor of the greater sampling density in ECS-3, as mentioned earlier.

Trace Metals

Trace metals, from natural and anthropogenic sources, are commonly enriched in reservoir sediments when compared to soils, as they can adsorb to fine-grained sediments that are ultimately deposited in low energy environments such as reservoirs (Long *et al*., 2002). Therefore the increase in Ba, Cd, Pb, and Zn concentrations in ECR reservoir sediments is likely due to association with soil runoff, when compared to soils (Figure 10). The high correlations between metals are a factor of this physical process.

The sedimentation history of Cu in ECR is important as it speaks to the high concentrations of Cu in sediments due to Cutrine Plus treatments in the upper sections core. Copper concentration peaks are only noted in the top ~10 cm of each core (when considering soil sediments and reservoir sediments only). Reservoir Cu concentrations increase up to 3-fold in the top ~10 cm in each core.

Average Cu concentrations were lower than averages determined by the surficial sediment study of 2002 in ECR (Tedesco *et al.,* 2003) (Table 3). The higher surficial

sediment study averages are attributed to the sampling strategy, where 97 surficial samples were collected in 2002, while the cores represent two distinct points within the reservoir, directly below treatment areas. Therefore, for comparison, the average Cu concentrations of upper core sediments from ECS-3 were compared to the 2002 surficial sediment results from three sample sites located in the same area. Average Cu concentrations for the top 10 cm of ECS-3 was about 46 μg/g, and the average of the three surficial data points collected form the same area in which ECS-3 is located, was 69 μg/g. This evidence supports the idea that ECS-3 Cu concentrations are more representative of one specific point, whereas the 2002 surficial study averages represent a more whole-reservoir view of Cu. However, the data shows that the copper that is applied to the reservoir is largely retained in the reservoir sediments.

Copper concentrations in the algaecide-treated Wisconsin lakes and Lake Erie are slightly higher (100 μg/g, Hutchinson, 1975; 100 μg/g, Stumm, 2001, respectively) than those found in this study, and others by Lwanga *et al*., 2003 (13 μg/g) (Table 8). Copper concentrations found in Northern Indiana wetlands (17-150 μg/g) were also comparable or higher than those found in ECR (Table 8).

Cadmium concentrations are enriched in reservoir sediments, when compared to pre-flood soil concentrations (Figure 9). The downcore reservoir profiles are very similar for both cores, and the minimal concentration range is similar to that of Fe, from 11-13 μg/g in reservoir sediments, unlike P and S.

Cadmium concentrations are high when compared to four lakes in New Jersey and New York, which ranged from 0.5 to 1.6 μg/g (Long *et al*., 2002), and in sediments from

Lake Michigan (Table 8). The Cd concentrations were similar to those from the surficial sediment study conducted in ECR, GR, and MR (Table 3).

Barium sediment concentrations are higher in ECS-3, and in general are more variable than other metals, ranging from 100-300 μg/g in both cores. Reservoir sediment Ba concentrations agree with those recorded in surficial sediments from ECR, GR, and MR.

The down core profiles of Ba in lake sediments become slightly less variable with depth, indicating that Ba may be mobile in the top 20 sediments, as noted in the down core profiles of S and total P. The profiles are more similar to that of S and P than any other element, perhaps indicating that $BaSO_4$ may also be present in sediments and acts as an oxidant in the mineralization of OM. Further study of other intermediate metals such as calcium (Ca), magnesium, (Mg), or strontium (Sr), coupled with a more detailed study of S in sediments, may be a way to confirm the high concentration of S minerals capable of being used in organic matter decomposition by S-reducing bacteria.

The profiles of Pb concentrations reflect the depositional history of this largely anthropogenically deposited heavy metal (Figure 9). Concentrations between cores agree very closely with the decrease in atmospheric deposition of Pb that occurred in 1986. The ban on leaded gasoline and lead-based paints in the late 1980's is recorded in the decrease in Pb concentrations in the ECR Pb down core profiles, at about 25 cm in ECS-1 and 38 cm in ECS-3. As in the profiles of Fe and Cd, Pb concentrations show little variance and high agreement between cores, with the exception of must variability noted right after the organic-rich contact layer.

Lead concentrations in pre-reservoir sediments are comparable to those of the adjacent soils, which range from 24 to 58 μg/g (Filippelli, *et al*., 2005). Reservoir sediment Pb concentrations are also comparable to those found in surficial ECR sediments, and those found in the other central Indiana reservoirs GR and MR (Table 3). Stumm (2001) found sediment concentrations of 125 μg/g Pb in Lake Erie sediments; Chillrud (1999) recorded Pb concentrations of 26-650 μg/g; and Perkins (2000) documented a sediment Pb concentration range in Northern Indiana wetlands of 65-280 μg/g (Table 8).

Down core profiles of Zn are similar to P, S, and Ba, in that they show variability in concentration ranges. This indicates that Zn oxides or sulfides are present. It is also expected that Zn is present as a reflection of its use in automobile tires.

Zinc concentrations were comparable or lower than those of ECR, GR, and MR; and those determined in other urbanized lakes from Africa, 118 μg/g (Lwanga, 2000); reservoirs in New Jersey, from 67 to 11,800 μg/g (Long *et al*., 2002); as well as those reported Zn results from Northern Indiana wetlands, 95-1700 μg/g (Perkins, 2000) (Table 8). Zinc and lead deposits are both associated with automobiles (Callender and Rice, 2000; Long *et al*., 2002), yet leaded gasoline has been banned from use since 1986 whereas Zn is still used in automobile tires. This explains why a decrease is noted in Pb concentrations.

Figure 11 shows the relationships between Pb and Zn, Pb and Cd, and Pb and Ba. The metals are all used in industrial processes. As such, Pb is strongly correlated to Zn, Ba and Cd in reservoir sediments.

Correlations between Zn and P are identical to those of Cd and P in that they are moderately correlated in ECS-3 but strongly correlated in ECS-1 (Table 9). This may be due to redox chemistry in the deep basin, which would cause dissolution of oxides and therefore less correlation with P.

These agreements, between the timing of anthropogenic metal inputs (such as Cu and Pb), and sediment metal concentrations, indicate that the values calculated for sedimentation rates, though not representative of the entire reservoir system, are appropriate for each core. Therefore these rates may be used to determine the accumulation rates of different forms of P.

5.3 Phosphorus and oxygen cycling

Detailed P geochemistry for the ECR cores shows that Fe-P is the dominant form of sediment bound P. Iron-P, that which can be released into the water column by the dissolution of redox chemistry-controlled iron oxyhydroxides, is the form of concern upon remobilization in ECR, because it is also instantly bioavailable P when refluxed in the water column. Figure 12 shows that this trend in high concentrations of Fe-P has historically occurred in ECR sediments.

The P data are discussed in the order that the extraction technique isolates each fraction, as shown in Figure 12. Figure 13 shows the downcore data as percentages of total P. ECS-1 Fe-P varies between periods of around 1 and 0.6 mg/g. Fe-P concentrations in ECS-3 are always higher for the same time intervals and have a more regular variability between 1.2 to 1.6 mg/g. Finding higher concentrations in ECS-3 Fe-P is not surprising considering the previous results presented, most elemental concentrations are higher in ECS-3.

The Fe-P profile of ECS-1 is relatively stable within the top 15 cm, suggesting that a process is occurring here that inhibits any substantial loss or gain of Fe-P. A similar process is document by Campbell and Trogersen (1980) as the “ferrous wheel”, a phenomenon observed in reservoir sediments, in which Fe that is dissolved in anoxic hypolimnetic waters is reprecipitated in the oxic waters directly above, creating little change in Fe concentrations through time, much like the process outlined in Figure 2.

The Fe-P profile of ECS-3 decreases down core, suggesting that Fe-P does migrate, possibly from saturated pore water mobilization by bioturbation, or another mixing process, due to redox chemistry in the anoxic layer. This decrease is probably due to the persistent loss of Fe-P from the iron redox cycling. This suggests that the Fe-P rich hypolimnic waters are mixed and available for nutrient use. Further study into the water chemistry in this area would be needed to determine the kinetic constraints on this process.

Iron-P and O-P fractions show notable differences between cores, within the top 8 cm. While ECS-1 Fe-P concentrations slightly decrease from the surface, from about 1.0 mg/g to 0.7 mg/g (30% decrease), ECS-3 Fe-P concentrations decrease from about 1.8 mg/g to 1.3 mg/g (26% decrease). At the same time, O-P fractions in ECS-1 decrease from about 0.27 mg/g from the surface to about 0.23 mg/g (15% decrease), while O-P values reach a decrease from about 0.35 mg/g to 0.29 mg/g in ECS-3 (17% decrease). Based on the similarity of relative percents of decrease in Fe-P and O-P, these data indicate that Fe-P is being released during periods of anoxia in both cores, to 8 to 10 cm depth. The greater down core decrease in Fe-P noted in ECS-3 agrees with the hypothesis

that anoxic periods are long enough in the deep basin to cause greater amounts of dissolution of Fe-P.

Although the data suggest that iron redox cycling is at work in ECR, thereby adding fuel for algal blooms, the decrease in Fe-P and O-P down core could be a result of natural organic matter mineralization processes. However, based on other study data that shows sediment-water interface flux can occur as deep as -20cm (Larsen *et al*., 1981; Song and Muller, 1999), the top ~15 cm is the apparent "depth of influence," with regard to sediment P cycling. After that depth, the profiles show the affects of early diagenesis, although ECS-3 O-P concentrations remain slightly higher (Figure 12).

Authigenic-P (A-P) concentrations are markedly higher in ECS-3 than in ECS-1 (about 3 times), yet Detrital-P (D-P) concentrations are nearly identical for both cores. Figure 13 shows that the relative percent of A-P is slightly lower in ECS-3. Therefore the greater amount of A-P in ECS-3 is not an anomaly.

Generally, ECS-1 has a higher O-P fraction than that of ECS-3 but a slightly lower fraction of Fe-P. These same trends do not change through time (Figure 13).

Correlations between the various P fractions reveal further clues to the differences in the processes that occur at the sediment-water interface at different water depths in ECR. Correlations between Fe-P, O-P, and reducible Fe are stronger in ECS-1 than in ECS-3 (Figure 14). Based on the previous data presented, the correlations in ECS-3 are lower due to longer periods of anoxia in the deep basin. As expected, there is a strong correlation between Fe-P and reducible Fe in ECS-1 (R=0.90, Table 9), due to the adsorption of P to Fe-hydroxides (Figure 14a). Though there is a moderately strong correlation in ECS-3 (R=0.61); the difference is probably due to more efficient iron redox

cycling at the 7 m water depth (ECS-1), in which concentrations are kept in check by the constant cyling. In the case of ECS-3, the 16 m hypolimnia appears to be influenced by anoxia and Fe cycling, but Fe-P and reducible P are less correlated (ECS-3) (Campbell and Torgersen, 1980). This disassociation may be attributed to release of Fe-P into the photic zone, which is quickly utilized in the metabolic processes of nuisance bacteria, thereby restricting the dissolved Fe-P from rebinding to Fe. Further data on the sediment-water interface characteristics of the 16 m portion of the reservoir are needed to support this hypothesis

Organic P is strongly correlated to reducible Fe in ECS-1 (R=0.71), but not at all correlated in ECS-3 (Figure 14b; Table 9). This difference speaks again to the occurrence of the iron redox cycle in ECS-1, where the dissolution of sediment bound P is constrained by oxic conditions.

The difference in correlations in ECS-3 is due to concentrations of O-P increasing while Fe-P concentrations remain relatively constant. This occurrence of increasing O-P is probably a function of increased algal sedimentation in the deep basin. Finally, a strong correlation exists between O-P and Fe-P in ECS-1 (R=0.70) but not at all in ECS-3 (Figure 14c; Table 9). Partially this difference is inferred as increased algal sedimentation in deep core, but this data also speaks to the possibility of the "ferrous cycle" leading to a loss of Fe-P in the deep basin. The values are more scattered for ECS-3, and Fe-P is only slightly correlated to reducible Fe (R=0.38), suggesting that anoxia and the related chemical interactions drive the dissolution of iron oxides, resulting in a dis-proportionate amount of reducible Fe in the sediments.

The relationship between O-P and reducible Fe, and the relationship between O-P and Fe-P, are similar in distinct ways in both cores. Organic-P is only moderately correlated to reducible Fe and Fe-P (R=0.50) in both cores, but the data points are concentrated in two distinct groups. There is no correlation between either O-P and reducible Fe, or O-P and Fe-P in ECS sediments. The grouping that is noted in ECS-1, but not in ECS-3, suggests that the different water depths do have an affect on the depositional patterns of the three elemental fractions.

Concentration differences in reducible Fe and Mn, act as further indication that different sediment-water interface regimes are present (Figure 15). Like the other metals, concentrations of reducible Mn are greater in ECS-3 than in ECS-1; however, the concentrations of reducible Fe in EC-3 are about 0.5 wt% less than those in ECS-1. The decreased concentration of reducible Fe in ECS-3 suggests that the dissolution and subsequent flushing of dissolved Fe is occurring in the deep portion of the reservoir (Fe-P would also be released).

Reducible Fe is one of the few elements displaying lower concentrations in ECS-3 than ECS-1 (Figure 15). This difference is attributed to the dissolution processes, either chemically or biologically reduced, that appears to occur in the top 10 cm of sediment in the deep basin.

As mentioned above, the highest concentrations of Fe-P and O-P in ECS-3 are seen during the last 5 years, or roughly the top 10 cm of sediments. However, Figure 16 shows Fe-P and O-P as accumulation rates. During the time of CP treatments, Fe-P concentration rates are becoming more similar, indicating that the surficial treatments of

algaecide are actively controlling the algal blooms. Organic-P rates are also decreasing in ECS-3, but rates in ECS-1 have been increasing since the treatments.

Roden and Edmonds (1997) suggested that the combination of FeS was the reason the ferrous wheel could not chemically fuction in experimental cores, leaving the additional dissolved phosphate to become redistributed within the water column above the sediments (Figure 17). Anaerobic sediments containing sulfate-reducing bacteria release hydrogen sulfide, which is then bound to available Fe(II). This could be the case in ECR, in the deep location where calm waters and high organic matter contents allow for anoxic conditions. This new anaerobic environment promotes further reduction of organic matter and redox potentials, and release of oxide-bound P. If the reduced iron binds to sulfur to form FeS, the previously bound P would slowly permeate to upper surface waters. Concentrations of sulfur decrease by half in the top ~12 cm of ECS-3 (Figure 8). Iron shows a slight decrease, but small changes would be better noted in less abundant elements.

Eventually, the dissolved phosphate in the hypolimnetic waters could become mixed into photic zones rapidly during high-volume mixing events such as the Labor Day flood that occurred in ECR on September 1, 2003. Based on readings of O-P in hypolimnetic waters from August 2003, collected as part of a hypolimnetic dissolved-P study conducted by D.L. Pascual, this dissolved P exists in stagnant summer hypolimnia. This process would suggest that as time goes on, concentrations of Fe-P will continue to look much the same, but O-P will increase as the sediment-water interface is now laden with enough reducible oxide-bound P to influence the biological productivity of the reservoir.

Data retrieved from sequential extractions of P were compared to the DO, specific conductivity, and temperature of the ECR water column for 2003 to suggest a possible scenario for the flux of bioavailable P in ECR. In the middle of August the reservoir was thermally stratified, with differences in surface and at depth temperatures of around 5-10^{o}C. Dissolved oxygen readings were zero to 2 mg/L up to an average of 4 m from the reservoir bottom. During this same period, a prolonged, high reduction potential was recorded (-50 to 50 mV), capable of dissolving Fe-P. This entire anoxic system was disrupted by a flood that occurred on September 1st, when the water column became mixed. It is this process that could be responsible for the redistribution of bioavailable P into the photic zone in the late summer of 2003.

Similar studies of the fractions of reservoir sediment P concentrations were conducted in Sweden (Boström *et al*., 1988) where data suggested that lakes with different trophic levels displayed distinct characteristic fractions of P (Table 8). Nürnberg (1984) discovered that lakes rich in iron and humic material represented lakes with high P retention capacity, as noted in the high percentage of oxide bound P (62%). ECR sediments matched these fractions closely, indicating that it was similar to this type of lake.

With sediments containing up to 77% Fe-P in areas experiencing potentially high periods of anoxic conditions, ECR has potential fuel for future algal blooms. Data suggests that the threshold levels are somehow related to concentration depth.

6. CONCLUSIONS AND IMPLICATIONS

In general, most elemental concentrations are greater in the deeper basin core (ECS-3) than in the core taken from the shallower water depth (ECS-1); with the notable exception of reducible Fe-P and O-P concentrations. Detailed P geochemistry reveals that Fe-P is the dominant fraction of P, similar to that of other eutrophied reservoirs (Boström, *et al*., 1988; Song and Muller, 1999). The Cu applied to the reservoir as an algaecide is almost entirely retained in the sediments.

The cores extracted from ECR in November of 2003 reveal a representative history for the entire reservoir. The anthropogenic history of the last 40 years is recorded in the sediments. The study concentrated on analysis of sediment P fractions and metals analysis to look at the major players in P flux at the sediment-water interface in ECR. It appears that the factors involved, around 10-12% organic matter, high oxide-bound P concentrations, and stratification, have been documented in other lakes with similar levels of eutrophication. The data collected from ECR adds to a growing list of studies on reservoir health. The sediment health of ECR, based on the two cores analyzed, rests on fractions of bioavailable P occurring within areas with a high risk of prolonged anoxia, either as a function of direct chemical reduction or indirect microbial reduction.

Based on sediment Cu concentration calculations, the Cu within algaecides is permanently stored in the reservoir sediments. Treatments have created increases in Cu concentrations of up to 3 times background reservoir sediment concentrations. The history of Pb use was recorded in the core and acts as an additional time marker. Most of the sediment concentrations of other anthropogenically produced trace metals were comparable to other lake sediments.

High sediment organic matter content, up to 77% Fe-P, and reservoir water thermal stratification indicate that potential for P dissolution continues to be high in ECR, and the sediment-water interface in ECR includes interactions to -15 cm. Remediation efforts may include sediment management procedures such as aeration in the deepest portion of the reservoir. As indicated by data retrieved from ECS-1, the natural iron cycling that occurs in lakes between an anoxic hypolimnia and an overlying oxic boundary does not appear to effect the dissolved P concentrations in the water column, at water depths to 7 m for ECR. Regular monitoring of temperature and DO at this location would be best to define periods of anoxia. However, the process can persistently produce dissolved P at water depths greater than 7 m when dissolved oxygen is depleated.

Future investigations into the physical and chemical characteristics of the deep basin, including time of anoxia, and water stratification with depth, are needed. A detailed examination of *in situ* sediment-water interface processes would fill in the current data gaps revealed at the termination of the study.

TABLE CAPTIONS

Table 1. Average climate and physical parameters of ECR.

Table 2. The history of Cutrine Plus applications to ECR since 2000.

Table 3. Surficial sediment sample concentration ranges and averages. All concentrations are reported in units of μg/g sediment, except for Fe and S which are in units of weight %, and P which is in units of mg/g sediment.

Table 4. Sequential extraction technique for phosphorus determinations.

Table 5. ECR core lengths, sedimentation rates, organic matter content, dry bulk density (DBD), moisture content, and water depths at site.

Table 6. Elemental concentrations, ranges, standard deviations, and typical detection limits. All concentrations and detection limits are reported in units of μg/g sediment except for Fe and S which are in units of weight %, and P which is in units of mg/g sediment.

Table 7. Summary of other geochemical and sequential P extraction studies.

Table 8. Concentrations and percentages of four P phases determined by sequential extraction.

Table 9. Elemental correlations for each core.

Table 1. Average climate and physical parameters of ECR.

ECR Physical Data

Constructed[a]	**1967**
Lake Surface Area (km^2)[a]	5.01
Bottom Surface Area (km^2)[b]	5.04
Maximum Depth (m)[a]	16.5

2002 Buoy Data		**Water Temperature (^oC)**	**DO (mg/L)**	**Conductivity (mV)**	**Turbidity**	**Average Climate**[c] (Humid Continental)
Winter (Dec 22-Mar 21)	mixed	5	12	>300	low	-2.7^{o}C, 6.4 cm ppt.
Spring (Mar 22-June21)	mixed	14	12	>300	mod-high	16.6^{o}C, 10 cm ppt.
Summer (June 22-Sept 21) **(stratified by late July)**	**top**	25	8 to 10	>300	very low	23.8^{o}C, 11cm ppt.
	>6m	18	<1	50 to -50		
Fall (Sept 22-Dec 21)	mixed	15	8	>300	mod-high	6.1^{o}C, 8 cm ppt.

a – Tedesco *et al.*, 2003
b – This Study
c – National Weather Service climate normals for 1970-2000

Table 2. The history of Cutrine Plus applications to ECR since 2000 (Tedesco *et al*., 2003).

Date	Km^2	Cutrine Applied (m^3)	Copper Applied (Kg)	Total Kg Cu/yr
2000				3,682
7/26-7/28	4.9	33.8	3682	
2001				3,565
5/17	1.6	10.4	1134	
6/21	1.6	10.4	1134	
9/7	1.6	11.9	1297	
2002				5,489
4/24	1.6	11.5	1247	
5/28	1.6	11.5	1247	
6/26	1.6	11.5	1247	
9/11	1.6	11.5	1247	
2003				4,371
4/30	1.6	11.5	1247	
6/11	1.6	11.5	1247	
7/25	0.82	5.8	629	
10/16	1.6	11.5	1247	
Total Cu				**17,106**
Average/yr				**4,276**

Table 3. Surficial sediment sample concentration ranges and averages. All concentrations are reported in units of μg/g sediment, except for Fe and S which are in units of weight%, and P which is in units of mg/g sediment (Tedesco *et al*., 2003).

	Element							
Reservoir	**Ba**	**Cd**	**Cu**	**Fe**	**P**	**Pb**	**S**	**Zn**
Eagle Creek								
conc. range	21-352	11-27	16-138	-	0.3-4.5	35-209	0.02-0.79	29-319
avg. conc.	168	21	66	-	1.9	129	0.4	177
Geist								
conc. range	33-306	9-15	2.7-24	0.7-3.9	0.3-4.0	25-119	0.04-0.91	19-219
avg. conc.	186	13	13	2	1.4	87	0.45	128
Morse								
conc. range	15-256	5-13	7-28	0.34-3.6	0.58-6	11-60	0.06-0.6	26-212
avg. conc.	67	5	8	1.1	3	21	0.17	77

Table 4. Sequential extraction technique for phosphorus determinations (Ruttenberg, 1992; Anderson and Delaney, 2000).

Step Name	Sequential Treatments	Reaction Process	P component isolated
Oxide-Reducible and Loosely Bound (Fe-P)	10 ml CDB solution (6 hr) (0.22 M sodium-citrate, 0.11 M $NaHCO_3$, 0.13 M sodium-dithionite) 10 ml 1 M $MgCl_2$ (2 hr) 10 ml H_2O (2 hr)	Reduction of Fe^{3+} by dithionate and subsequent chelation by citrate	Reducible or reactive iron-bound phosphate
Authigenic/ Biogenic (A-P)	10 ml 1 M Na-acetate buffered to pH 4 w/acetic acid (5 hr) 10 ml 1 M $MgCl_2$ (2 hr) 10 ml 1 M $MgCl_2$ (2 hr) 10 ml H_2O (2 hr)	Acid dissolution at a low pH	Carbonate fluorapatite (CFA), biogenic hydroxyapatite
Detrital (D-P)	13 ml 1 N HCL (16 hr)	Acid dissolution at a very low pH	Detrital fluorapaptite bound phosphate
Organic (O-P)	1 ml 50% (w/v) $MgNO_3$, dry in low oven, ash at 550^oC 13 ml 1 N HCL (24 hr)	Dry oxidation of organics; acid dissolution	Organically bound phosphate

Table 5. ECR core lengths, organic matter content, dry bulk density (DBD), moisture content, and water depths. Locations of core sites shown on Figure 4.

Core	Total Length (cm)	Compaction (%)	Water Depth (m)	Organic Matter (wt%)	Dry Bulk Density (g/cm^3)	Moisture Content (%)
ECS-1	55	28	7.2	2.9-11.5	0.38-1.48	16-69
ECS-3	109	34	16	1.9-12.2	0.27-1.68	17-76

Table 6. Elemental concentrations, ranges, standard deviations, and typical detection limits. All concentrations and detection limits are reported in units of ug/g sediment except for Fe and S which are in units of weight%, and P which is in units of mg/g sediment.

Element	ECS-1 Range	ECS-1 Avg.	ECS-3 Range	ECS-3 Avg.	Average std. dev. (%)	Typical Detection Limit[a]
P	0.935-2.43	1.81	0.651-3.31	1.81	2	0.017
S	0.084-0.455	0.249	0.142-0.840	0.329	5	0.013
Fe	1.91-6.44	4.85	1.12-14.3	5.89	2	0.030
Cu	6.75-47.4	20.6	9.53-67	33.18	5	0.004
Pb	8.47-62.0	42.9	7.29-69.6	40.0	11	0.02
Zn	66.2-220	162	75.6-278	171	8	0.001
Ba	3.54-213	153	3.64-276	156	2	0.001
Cd	6.68-13.3	11.2	7.65-13.7	11.5	3	0.002

a — Defined as 3 times the standard deviation of a blank sample

Table 7. Summary of other geochemical and sequential P extraction studies.

	Trace Metal Concentration (ppm)			
Location	**Cu**	**Cd**	**Pb**	**Zn**
Eagle Creek Reservoir[a]	6-67	6-13	7-70	66-278
Lake George, Uganda[b]	13	--	--	118
Allaquash Lake, Wisconsin[c]	25	--	--	--
Madison Lake, Wisconsin[c]	100	--	--	--
Lake Erie[d]	100	--	125	400
Packanack Lake, New Jersey[e]	--	1.5	400	450
Clyde Potts Reservoir, New Jersey[e]	--	0.5	110	300
Newbride Pond, Lond Island New York[e]	--	1.6	1000	10000
Orange Reservoir, New Jersey[e]	--	2	500	600
Lake Michigan[f]	--	1.3	26-650	80-450

a – This Study
b – Lwanga *et al*., 2003
c – Hutchinson, 1975
d – Stumm, 2001
e – Long *et al*., 2002
f – Chillrud, 1999

	Phosphorus Fractions (%)			
Location	**Fe-P**	**Mineral (A-P+D-P)**	**O-P**	**Total P (mg/g)**
Eagle Creek Reservoir[a]	69	12	19	1.8
Lake Vallentunasjon, Sweden[b]	22	17	61	1.8
Lake S. Bergundasjon, Sweden[b]	66	11	23	6.5
Lake Erken, Sweden[b]	12	38	50	1.2
Lake St.Hastevatten, Sweden[b]	7	2	91	0.95
Shagawa Lake, Minnesota[c]	47	14	39	1.8

a – This Study
b – Boström *et al*., 1988
c – Larsen *et al*., 1981

Table 8. Concentrations and percents of four P phases isolated by sequential extraction technique.

P Phase	ECS-1 Conc. mg/g	ECS-1 %	ECS-3 Conc. mg/g	ECS-3 %	AVERAGE % BOTH CORES
D-P	0.053	4.84 %	0.117	2.82 %	3.83 %
A-P	0.057	8.10 %	0.051	6.52 %	7.31 %
O-P	0.238	20.9 %	0.300	16.7 %	18.8 %
Fe-P	0.809	66.2 %	1.34	77.0 %	71.6 %

Table 9. Elemental correlations for ECS-1 and 3 reservoir sediments. Bold values indicate significance at 99% confidence.

Element Correlations: each core

Strong acid ECS-1

n= sample size

Element	P (n=46)	Fe	Cu	Pb	Zn	Cd	Ba	S	OM
P	--	0.14	0.26	**0.48**	**0.82**	**0.81**	0.27	**0.46**	0.33
Fe	--	--	0.03	0.12	0.16	**0.43**	0.13	0.01	**0.39**
Cu	--	--	--	0.22	0.35	0.32	0.36	**0.44**	0.36
Pb	--	--	--	--	**0.82**	**0.52**	**0.86**	0.32	0.04
Zn	--	--	--	--	--	**0.77**	**0.72**	**0.55**	0.30
Cd	--	--	--	--	--	--	**0.40**	**0.41**	**0.47**
Ba	--	--	--	--	--	--	--	**0.43**	0.11
S	--	--	--	--	--	--	--	--	**0.37**

Strong acid ECS-3

Element	P (n=66)	Fe	Cu	Pb	Zn	Cd	Ba	S	OM
P	--	0.03	0.25	**0.40**	**0.45**	**0.49**	**0.60**	**0.38**	**0.77**
Fe	--	--	0.19	0.09	0.06	0.04	0.07	0.01	0.20
Cu	--	--	--	0.07	0.12	**0.35**	**0.34**	**0.52**	**0.45**
Pb	--	--	--	--	**0.80**	**0.60**	**0.62**	0.17	0.20
Zn	--	--	--	--	--	**0.76**	**0.62**	0.17	0.31
Cd	--	--	--	--	--	--	**0.52**	0.30	0.04
Ba	--	--	--	--	--	--	--	**0.47**	**0.61**
S	--	--	--	--	--	--	--	--	**0.44**

Sequential ECS-1 (n=38)

Element	Oxide P	Red. Fe	Red. Mn	Org P	OM %
Oxide P	--	**0.90**	0.03	**0.70**	0.17
Red. Fe	--	--	0.12	**0.71**	0.07
Red. Mn	--	--	--	0.19	0.38
Org P	--	--	--	--	0.15
OM %	--	--	--	--	--

Sequential ECS-3 (n=38)

Element	Oxide P	Red. Fe	Red. Mn	Org P	OM %
Oxide P	--	**0.61**	**0.75**	0.08	0.18
Red. Fe	--	--	0.22	0.27	0.26
Red Mn	--	--	--	0.03	0.04
Org P	--	--	--	--	0.36
OM %	--	--	--	--	--

FIGURE CAPTIONS

Figure 1. The lake phosphorous cycle. Phosphorus is added to lakes in dissolved and particulate forms from natural weathering and agricultural and urban runoff. Most of this P is rapidly deposited in lake sediments where it will remain unless iron-rich sediments dissolve releasing P (Based on Wetzel, 2001).

Figure 2. Oxic-anoxic boundary transformation of Fe(II,III) in the water or sediment column. When water DO <1 mg/L iron dissolution becomes important to the coupled release of PO_4^{3-}(Modified from Stumm and Morgan, 1996; Wetzel, 2001).

Figure 3. Leaded and unleaded gasoline production between 1967 and 1991. The decrease in leaded gas production is partly due to the ban on leaded gas in 1986 (EPA, 1994).

Figure 4. Map of Eagle Creek Watershed with land cover distribution (Tedesco *et al.*, 2003). The land is generally flat to gently undulating glacial plains with slope angles of mostly 1-2% (Hall, 1990).

Figure 5. Bathymetry map of Eagle Creek Reservoir. The core locations for this study and the locations of the sampling points for the hypolimnetic water P study are identified on the map.

Figure 6. Core photo, description, moisture content, dry bulk density, and organic matter content for ECS-1.

Figure 7. Core photo, description, moisture content, dry bulk density, organic matter content, and magnetic susceptibility for ECS-3.

Figure 1. The lake phosphorous cycle. Phosphorus is added to lakes in dissolved and particulate forms from natural weathering and agricultural and urban runoff. Most of this P is rapidly deposited in lake sediments where it will remain unless iron-rich sediments dissolve releasing P (After Wetzel, 2001).

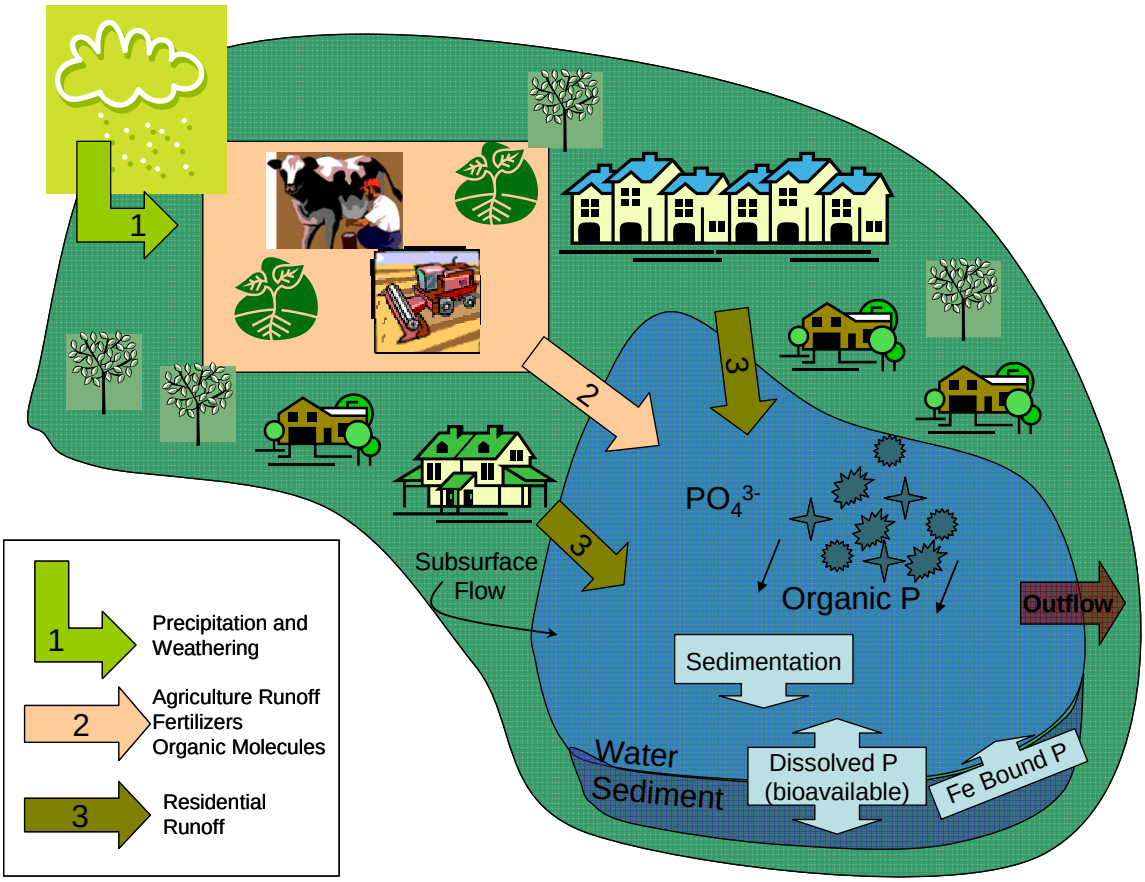

Figure 2. Oxic-anoxic boundary transformation of Fe(II,III) in the water or sediment column. When water has DO <1 mg/L, iron dissolution becomes important to the coupled release of PO_4^{3-}(Modified from Stumm and Morgan, 1996; Wetzel, 2001.)

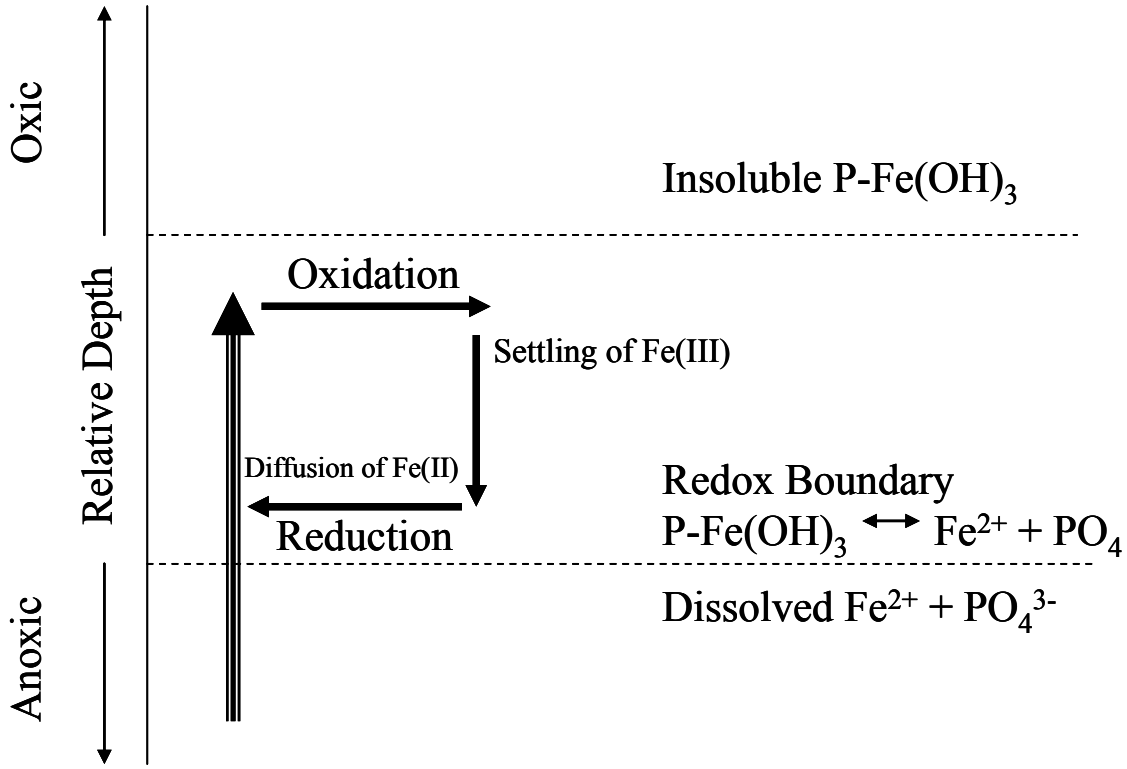

Figure 3. Leaded and unleaded gasoline production between 1967 and 1991. The decrease in leaded gas production is partly due to the ban on leaded gas in 1986 (From EPA, 1994).

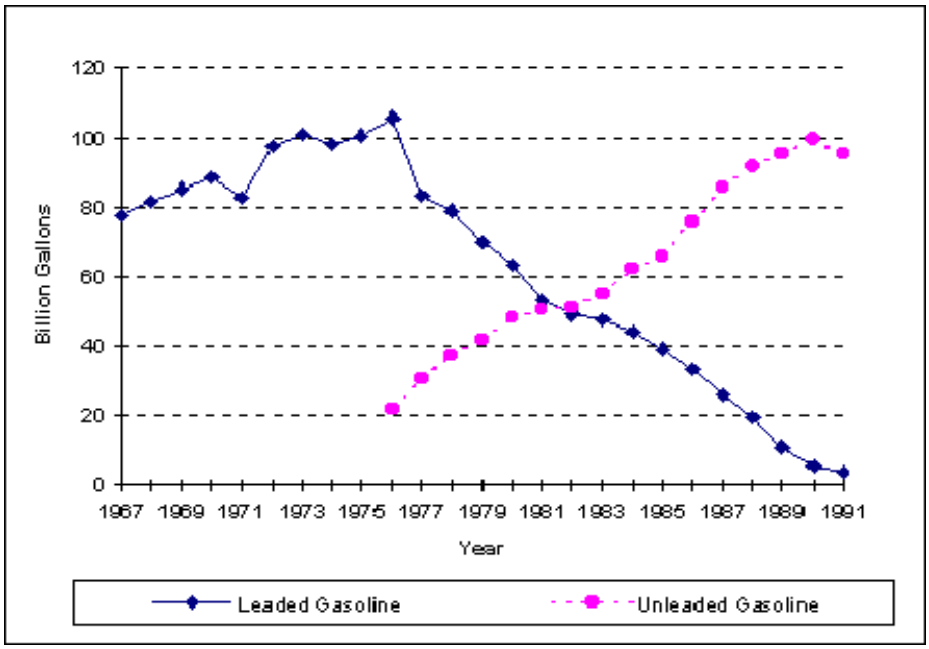

Figure 4. Map of Eagle Creek Watershed with land cover distribution (Tedesco *et al.*, 2003). The land is generally flat to gently undulating glacial plain with slope angles of mostly 1-2% (Hall, 1990).

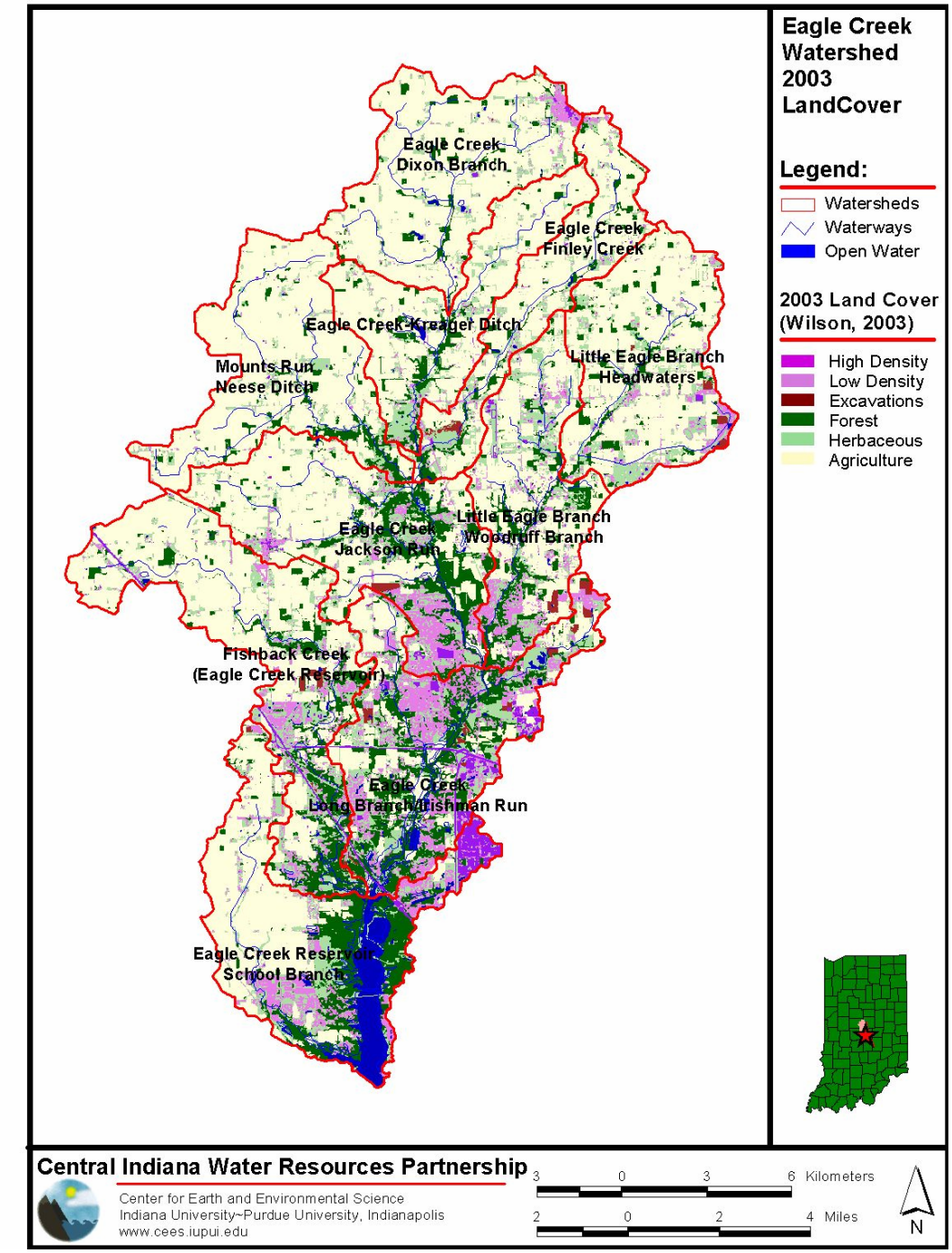

Figure 5. Bathymetry map of Eagle Creek Reservoir, with core sites ECS-1, and ECS-3. Hypo and buoy sites are complimentary data sets to be discussed. ECN-1 and ECS-2 will not be discussed.

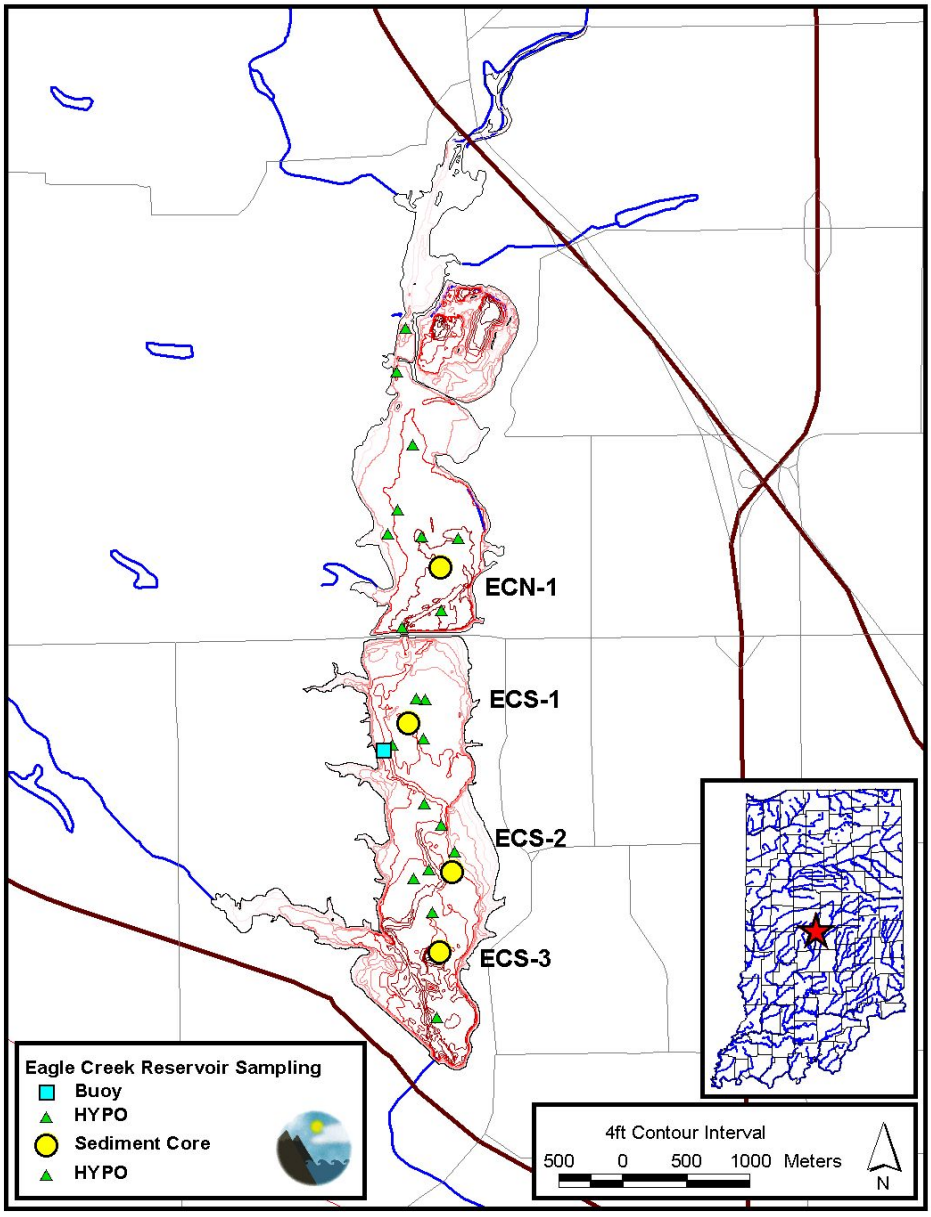

Figure 6. Core photo, description, moisture content, dry bulk density, and organic matter content for ECS-1.

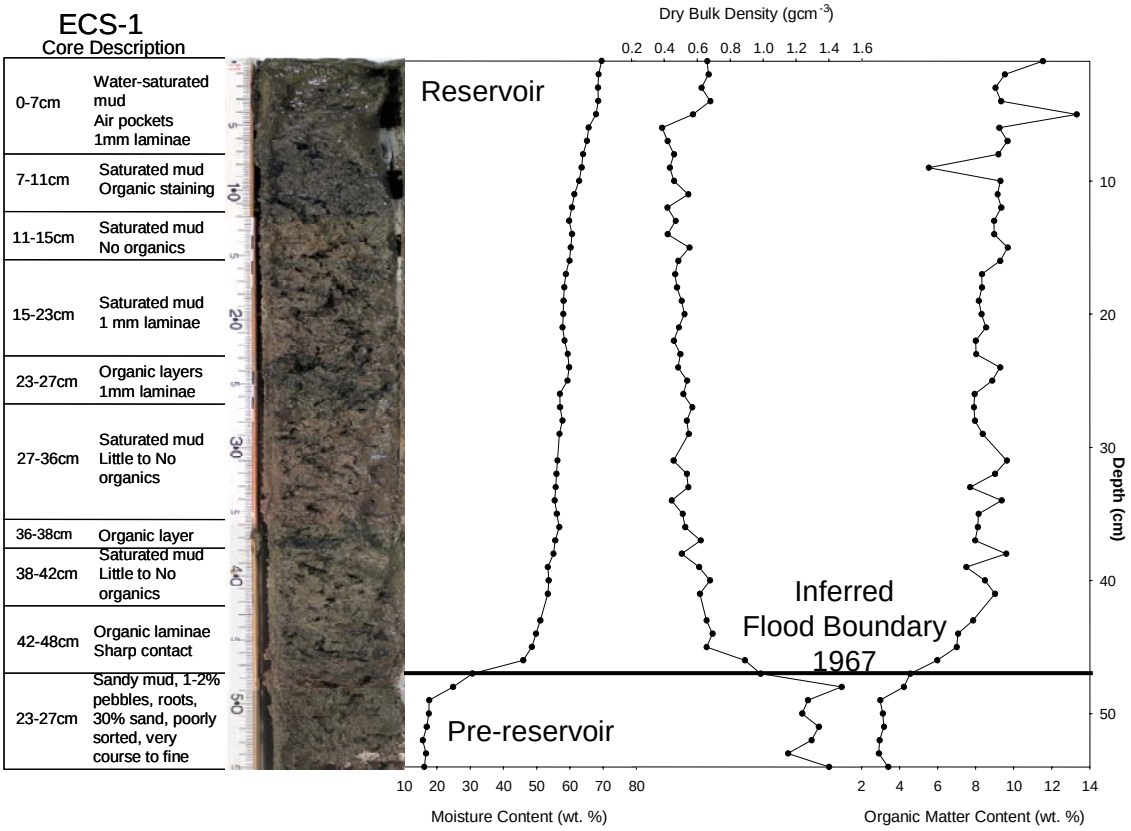

Figure 7. Core photo, description, moisture content, dry bulk density, organic matter content, and magnetic susceptibility for ECS-3.

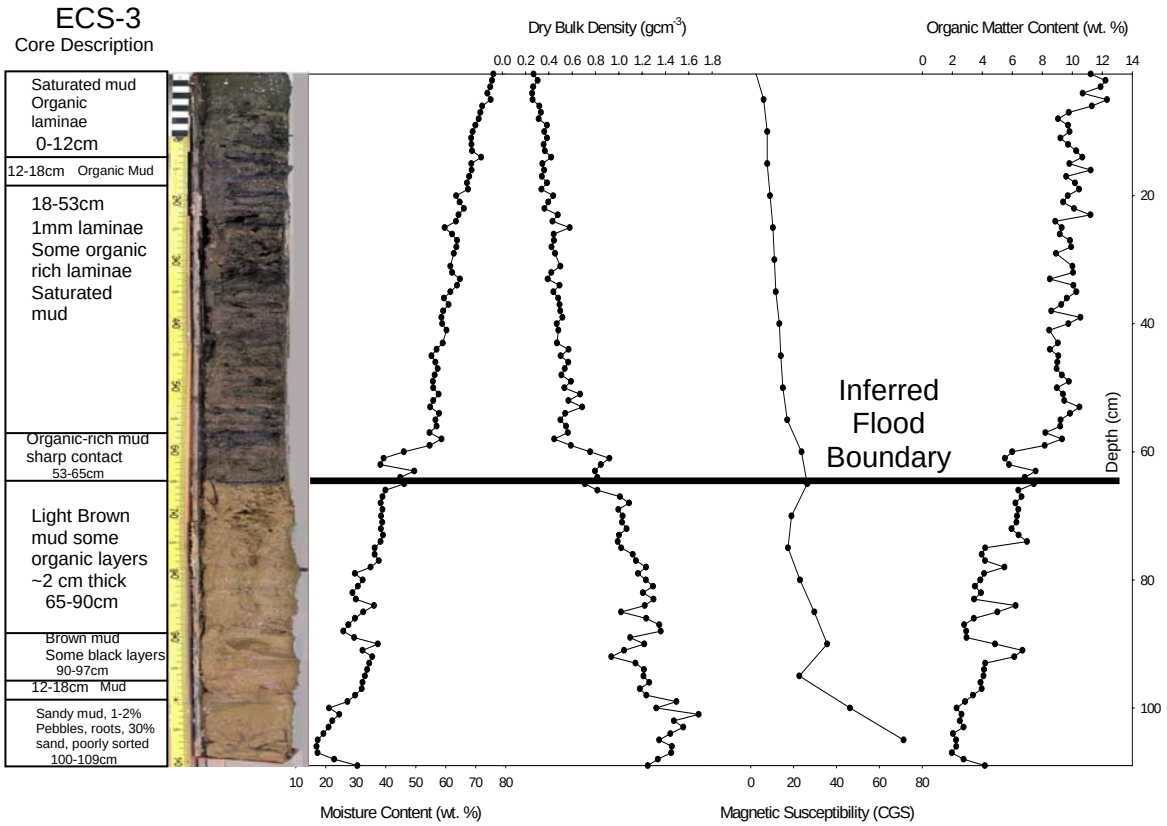

Figure 8. Total P, Fe and Sulfur geochemistry for ECS-1 and ECS-3 by strong acid determination.

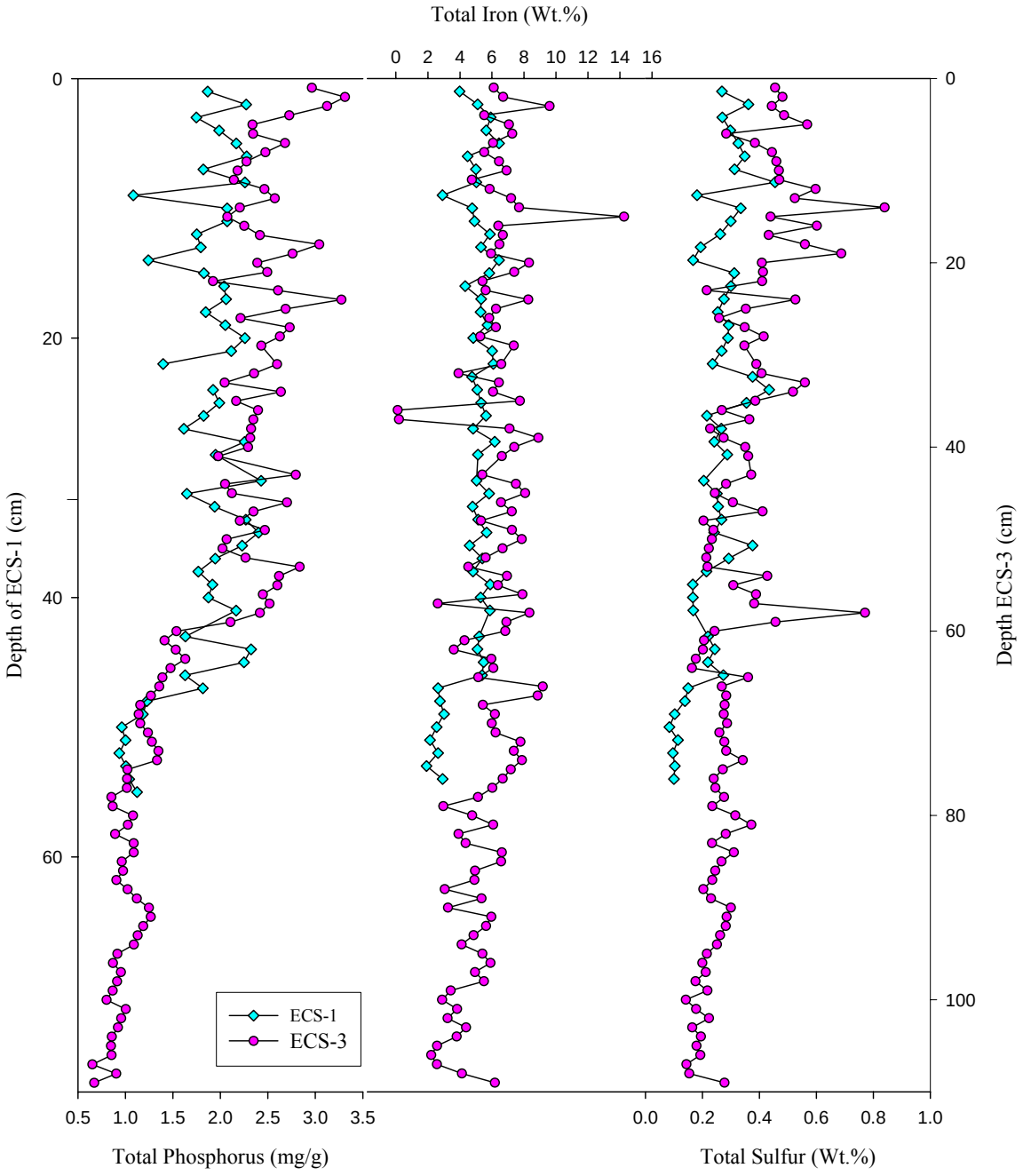

Figure 9. Metal Geochemistry for ECS-1 and ECS-3.

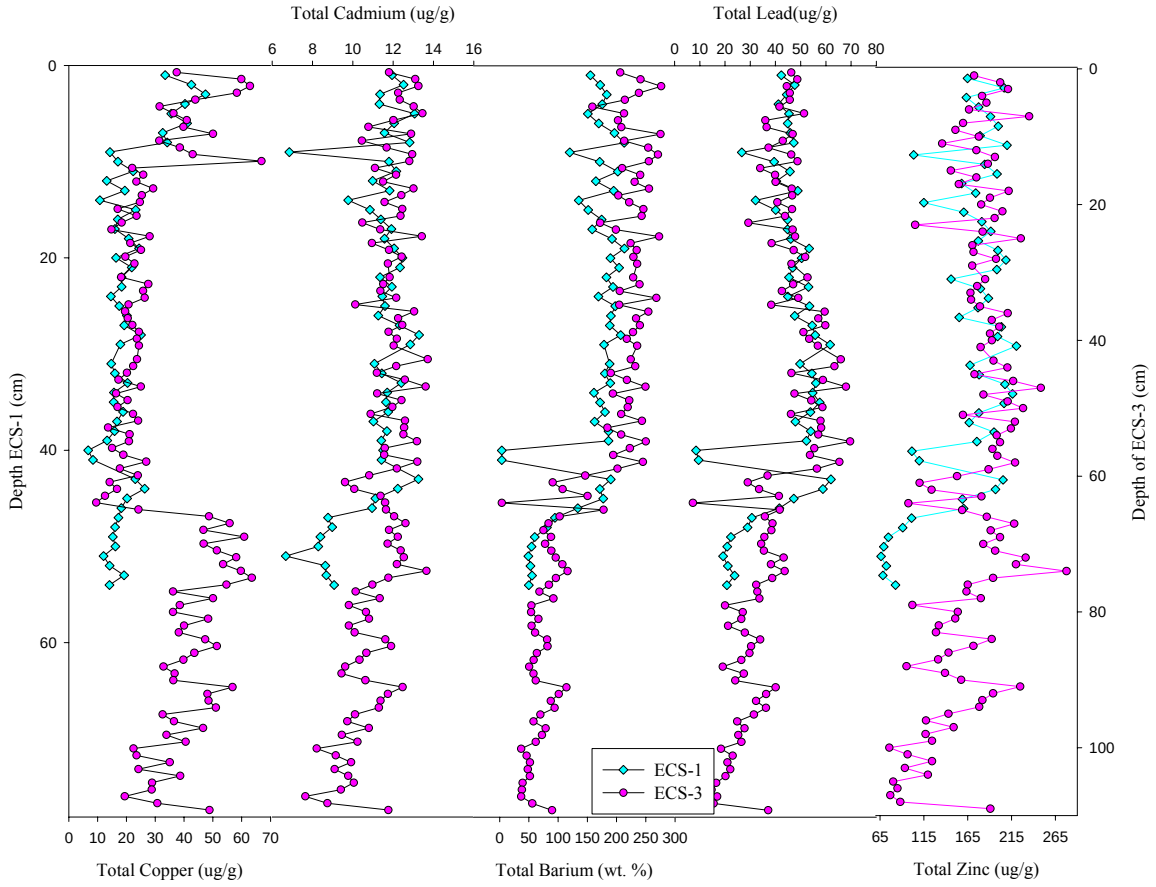

Figure 10. Relationships between a) organic matter and total phosphorus, b) organic matter and iron, and c) organic matter and sulfur in ECS-1 and 3.

a)

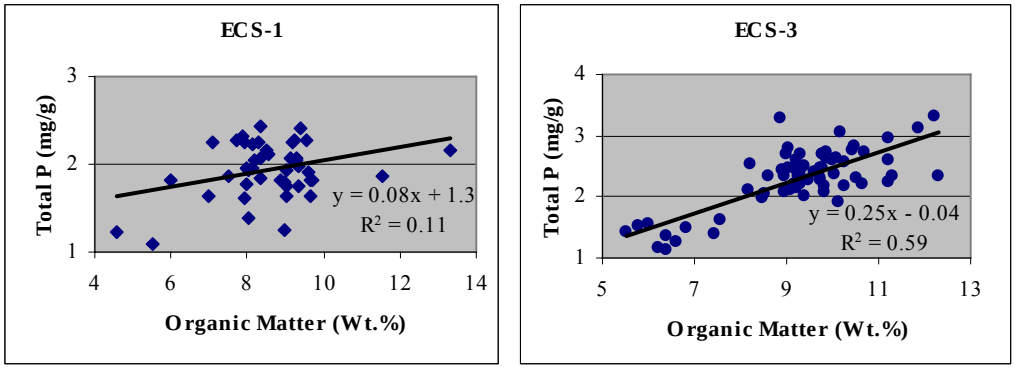

b)

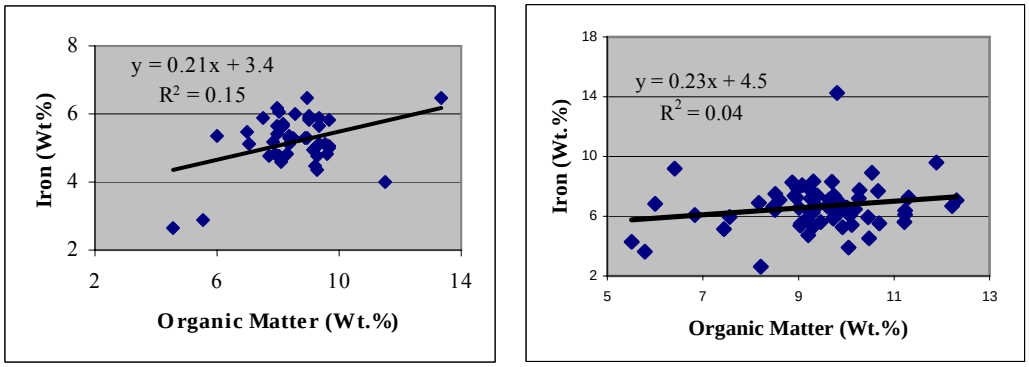

c)

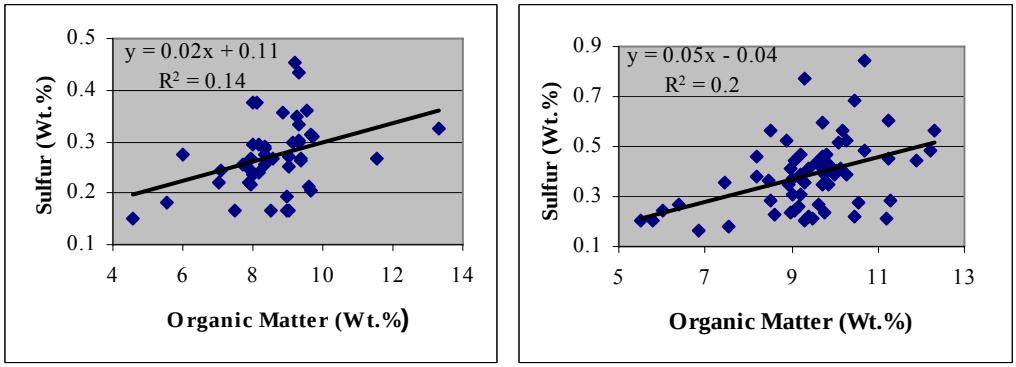

Figure 11. Relationships between a) zinc and lead, b) lead and cadmium, and 3) lead and barium in ECS-1 and -3.

a)

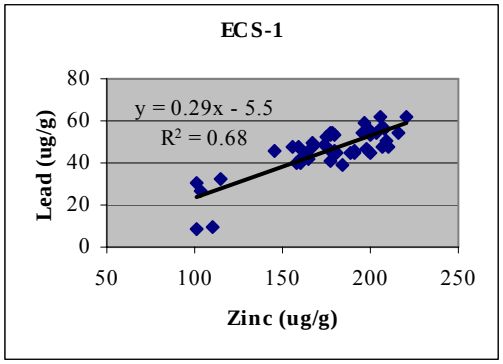

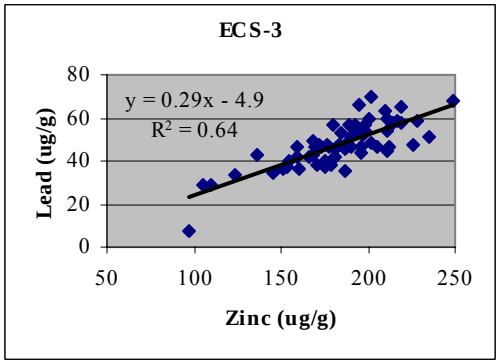

b)

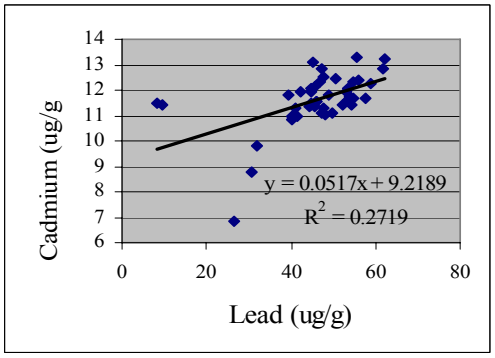

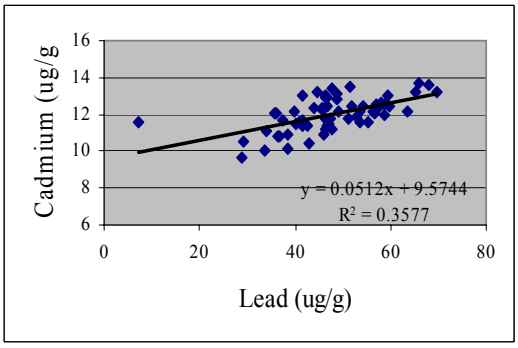

c)

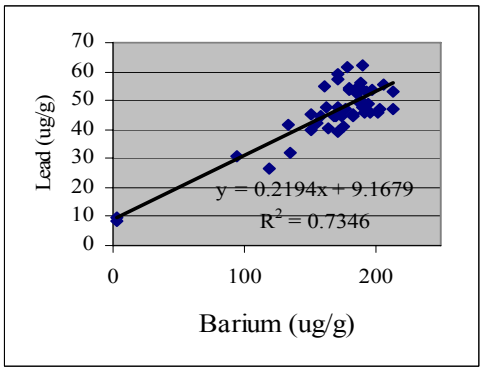

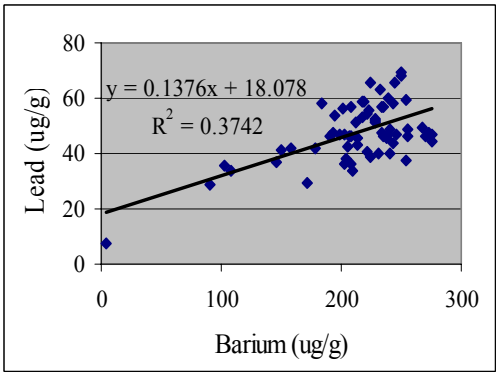

Figure 12. Detailed P geochemistry for post-reservoir sediments of ECS-1 and ECS-3: concentrations.

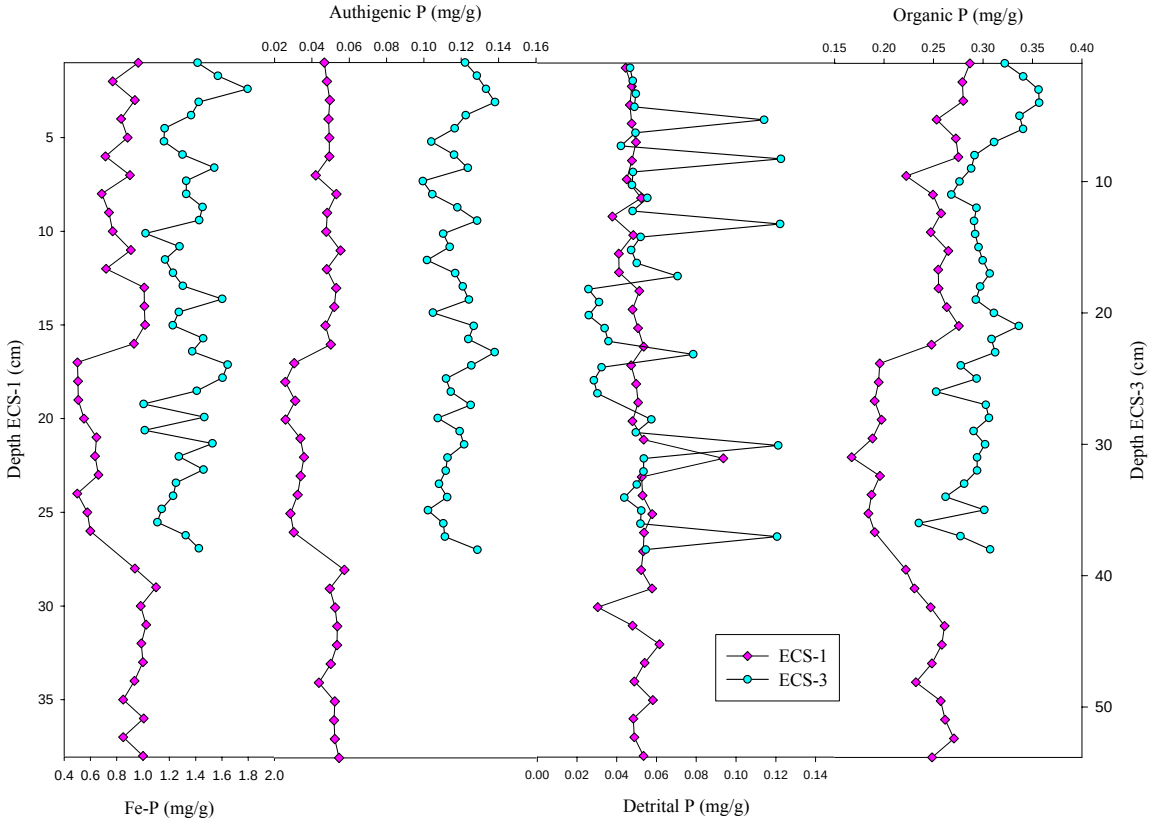

Figure 13. Detailed P geochemistry for post-reservoir sediments of ECS-1 and ECS-3: percentages.

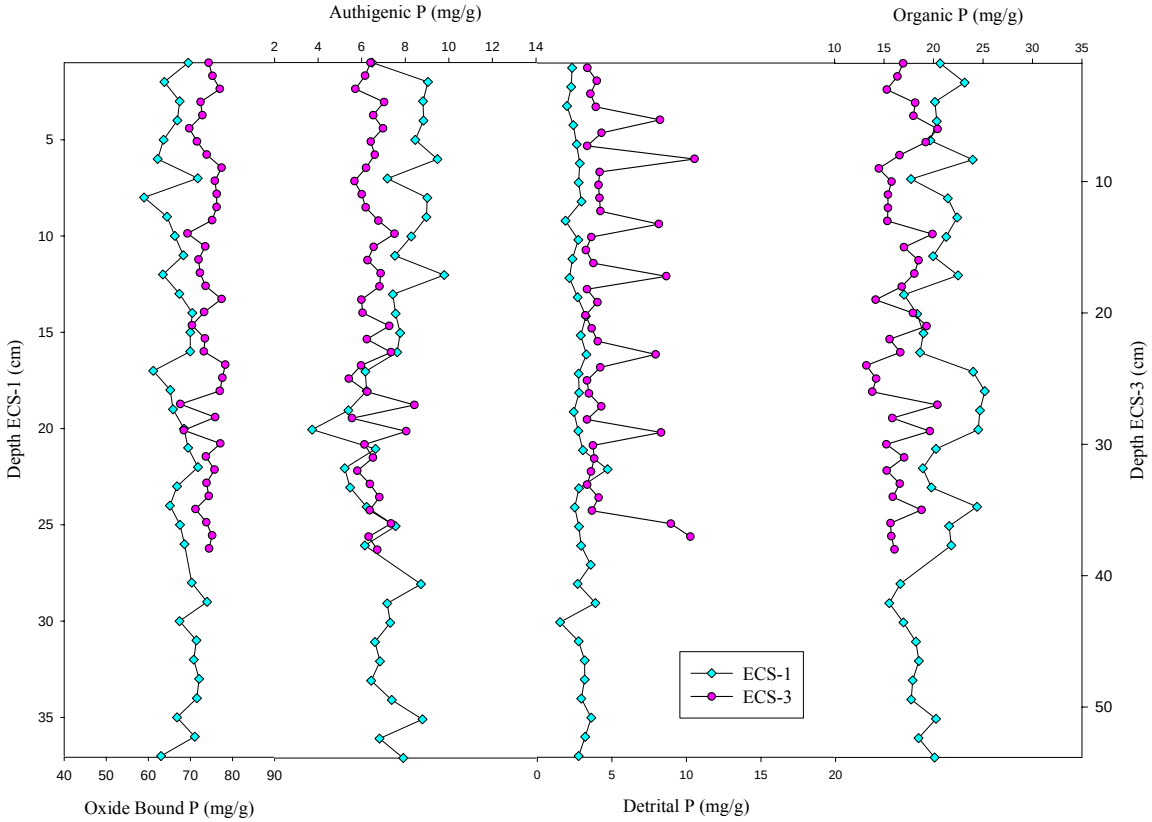

Figure 14. Relationships between a) reducible Fe and Fe-P, b) reducible Fe and O-P, and 3) Fe-P and O-P in ECS-1 and -3.

a)

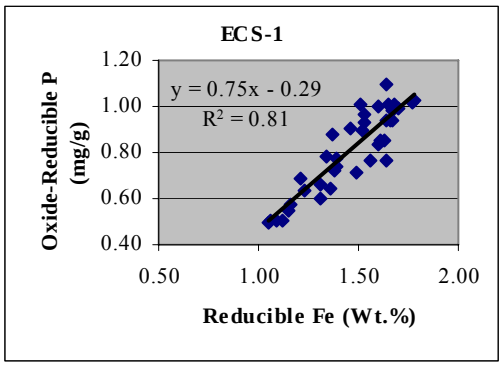

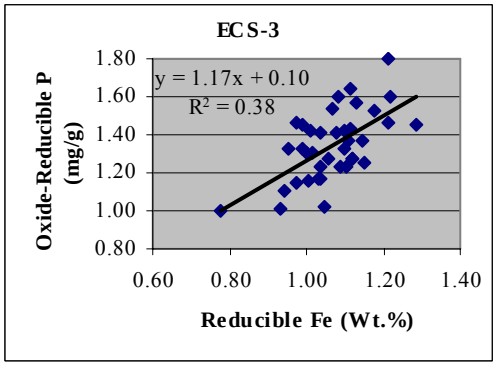

b)

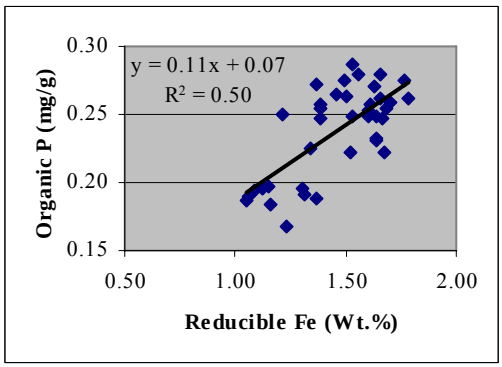

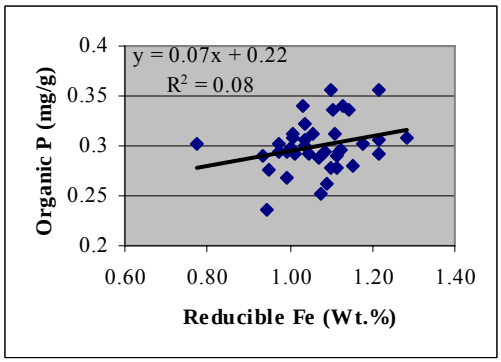

c)

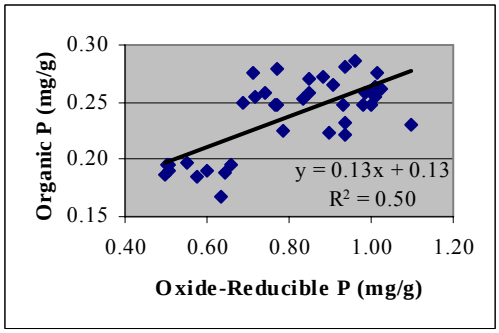

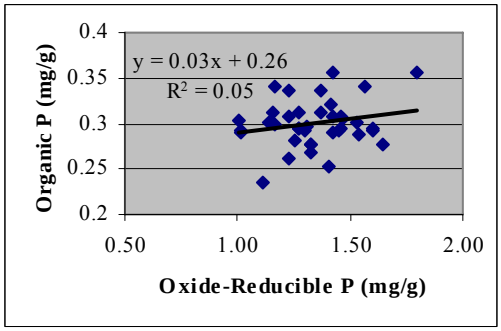

Figure 15. Reducible Iron and Manganese concentrations with depth to 38 cm.

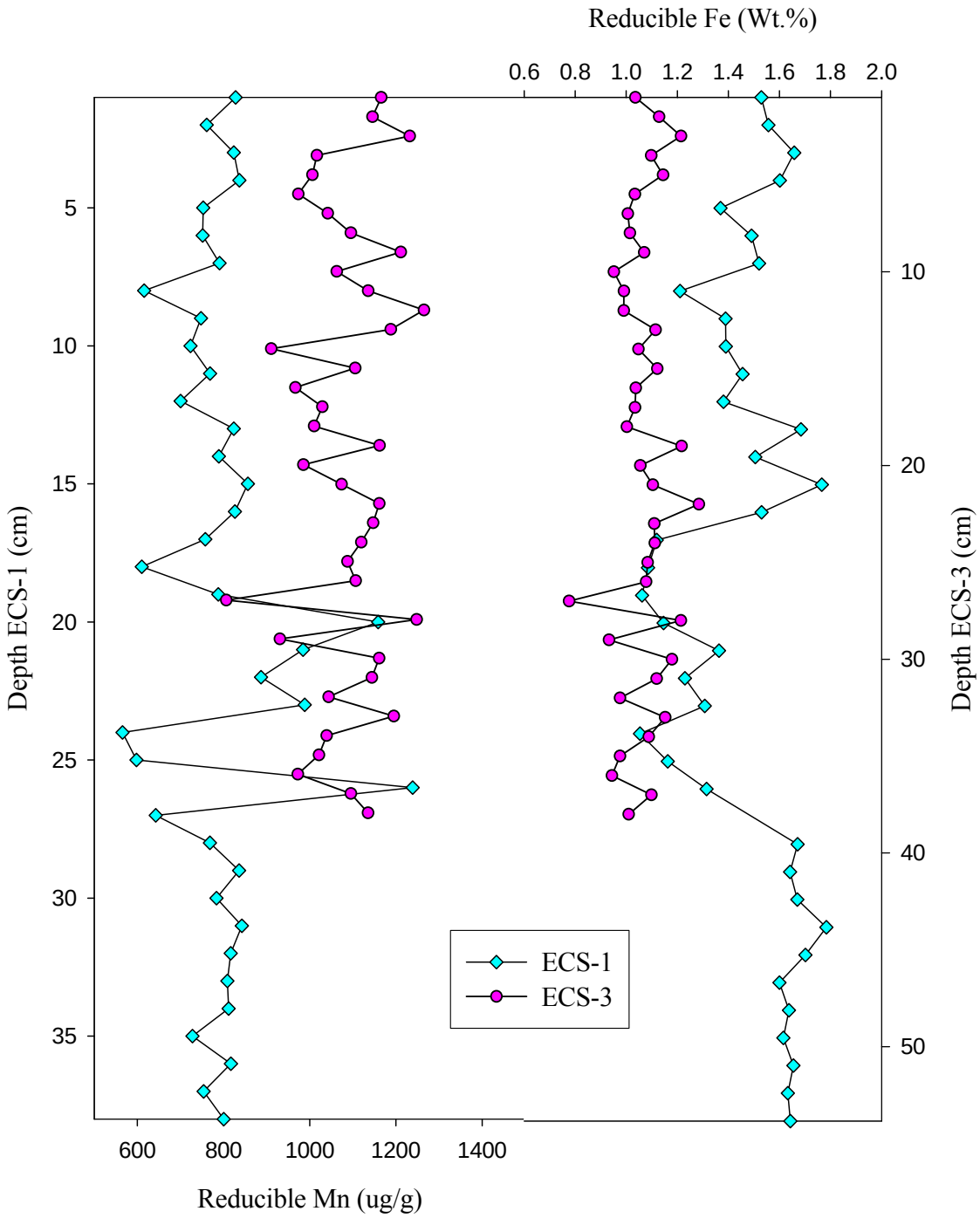

Figure 16. Accumulation rates for the O-P and Fe-P fractions.

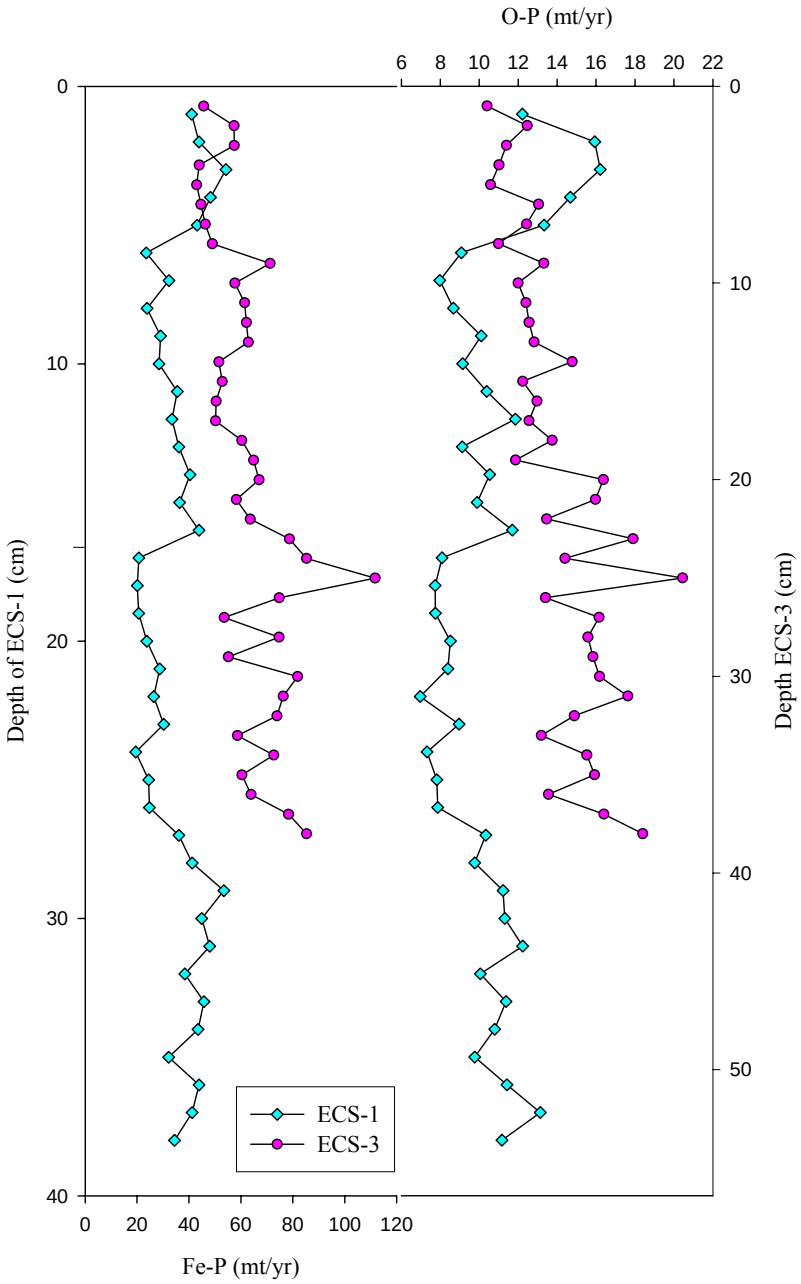

Figure 17. The Ferrous Wheel Process in ECR. The P cycle in ECS-3 when water becomes anoxic. The stratification of the water column creates what is commonly called a "ferrous wheel", in which Fe-oxides are dissolved and subsequently redeposited. If P is released, it is not available for redeposition. Furthermore, S may act as a binder to Fe to produce FeS_2. (Mondified from Roden and Edmonds, 1997).

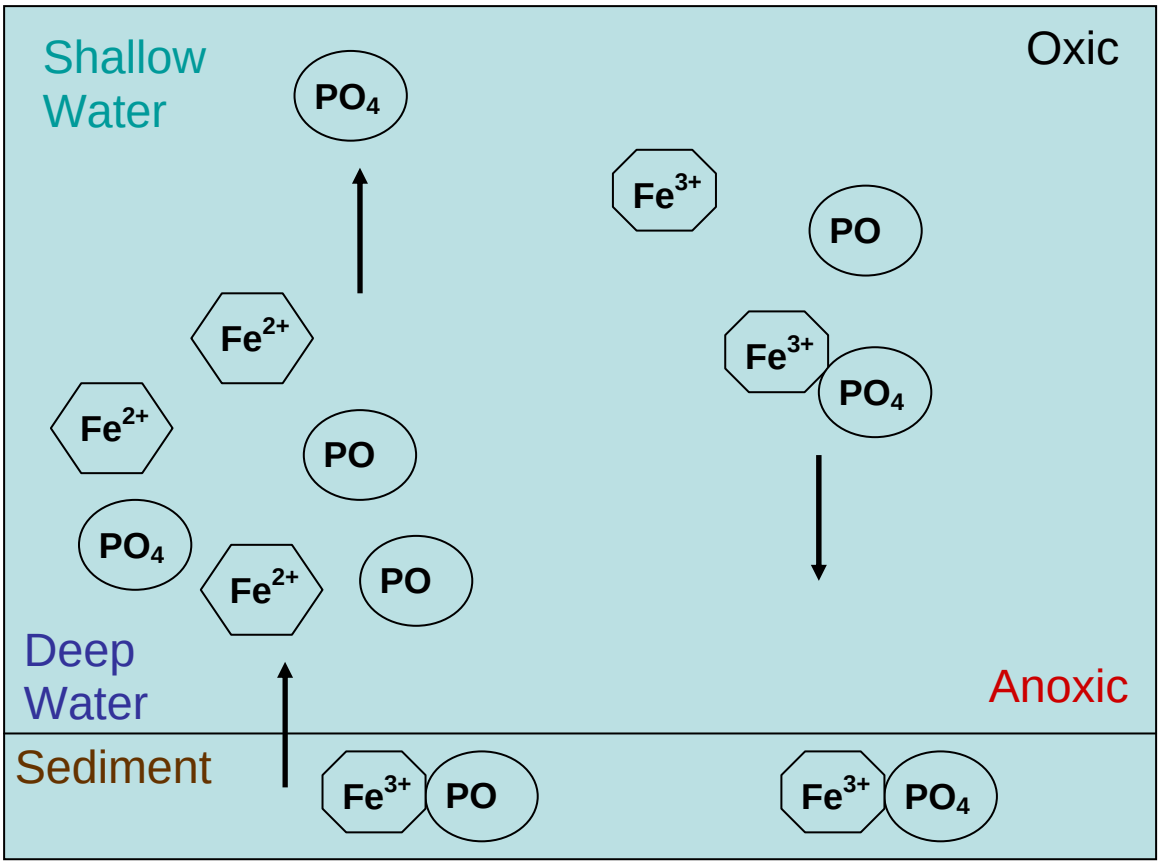

APPENDIX

ECS-1 (cm)	[P] (mg/g)	[S] (%)	[Fe] (%)	[Cu] (µg/g)	[Cd] (µg/g)	[Pb] (µg/g)	[Ba] (µg/g)	[Zn] (µg/g)
1	1.87	0.27	3.98	33.43	11.94	42.34	155.21	164.82
2	2.27	0.36	5.10	42.55	12.52	47.67	172.03	206.57
3	1.75	0.27	5.92	47.41	11.35	44.50	183.20	163.49
4	1.99	0.30	5.64	40.31	11.32	41.19	175.60	177.52
5	2.17	0.33	6.44	35.58	13.07	45.38	150.88	190.99
6	2.28	0.35	4.48	41.09	12.04	44.86	169.37	199.84
7	1.82	0.31	5.00	32.62	11.57	45.86	196.12	179.13
9	2.26	0.46	5.02	34.15	12.82	47.30	213.01	209.84
10	1.08	0.18	2.90	14.31	6.85	26.64	119.89	103.38
11	2.07	0.33	4.77	17.05	11.79	39.50	171.08	184.39
12	2.07	0.30	4.91	22.34	12.16	45.78	202.01	198.50
13	1.75	0.26	5.88	13.21	10.99	40.35	164.53	158.11
14	1.79	0.19	5.31	19.47	11.82	48.86	195.13	174.17
15	1.24	0.17	6.44	10.77	9.78	32.09	135.40	114.99
16	1.83	0.31	5.83	23.23	10.85	40.10	151.51	160.59
17	2.04	0.30	4.33	17.00	11.39	44.83	174.47	181.17
18	2.06	0.28	5.33	15.99	11.91	44.83	158.40	191.37
19	1.85	0.25	5.30	20.78	11.57	46.10	192.27	177.15
20	2.05	0.29	5.73	24.40	12.05	53.37	213.36	199.52
21	2.26	0.29	4.83	16.37	12.47	50.38	189.49	208.56
22	2.12	0.27	6.01	21.80	12.34	46.82	204.20	198.21
24	1.40	0.24	6.09	18.35	11.35	45.40	182.78	146.01
25	1.92	0.38	4.76	18.35	11.94	53.13	193.68	179.67
26	1.99	0.43	5.08	14.61	11.46	44.89	169.07	188.54
27	1.82	0.35	5.32	17.54	11.60	53.49	197.79	176.77
28	1.62	0.22	5.63	20.15	11.27	47.64	190.39	155.25
29	2.26	0.27	4.82	19.26	12.32	54.57	188.31	203.51
30	1.95	0.24	6.17	25.03	13.29	55.74	207.01	199.04
31	2.43	0.29	5.12	17.90	12.85	61.68	178.50	220.58
32	1.65	0.20	5.04	14.76	11.08	49.77	188.09	167.59
33	1.94	0.25	5.82	15.99	11.44	54.43	179.97	178.01
34	2.27	0.26	4.79	20.38	12.41	56.05	189.21	207.49
35	2.40	0.27	5.14	15.67	11.71	54.74	161.16	216.15
36	2.23	0.24	5.66	15.60	11.65	57.58	171.69	206.43
38	1.95	0.38	4.60	18.80	11.75	53.85	180.31	177.73
39	1.77	0.29	5.40	16.73	11.02	47.90	162.48	166.67
40	1.92	0.21	4.81	15.88	11.69	54.02	186.24	195.01
41	1.87	0.17	5.89	13.32	11.41	52.30	186.31	175.49
42	2.17	0.17	5.29	6.75	11.51	8.47	3.63	101.32
43	1.63	0.17	5.88	8.38	11.42	9.54	3.54	109.72
44	2.32	0.22	5.20	23.03	13.26	62.02	190.06	205.27
45	2.25	0.24	5.10	26.34	12.23	58.85	171.46	196.70
46	1.63	0.22	5.48	20.24	11.13	47.29	177.17	158.86
47	1.82	0.27	5.38	18.26	10.96	41.58	133.69	160.37

ECS-1 (cm)	[P] (mg/g)	[S] (%)	[Fe] (%)	[Cu] (µg/g)	[Cd] (µg/g)	[Pb] (µg/g)	[Ba] (µg/g)	[Zn] (µg/g)
48	1.22	0.15	2.63	17.24	8.77	30.64	94.64	101.01
49	1.18	0.14	2.75	16.10	8.98	28.94	80.97	90.86
50	0.96	0.10	3.01	15.30	8.39	22.34	59.87	74.59
51	1.00	0.08	2.54	16.17	8.29	20.91	54.56	69.28
52	0.93	0.11	2.13	12.04	6.68	19.26	49.02	66.19
53	1.01	0.10	2.63	14.19	8.64	21.11	52.57	72.20
54	1.04	0.10	1.91	19.18	8.69	23.80	55.35	68.28
55	1.12	0.10	2.92	14.12	9.07	20.71	49.73	82.68

ECS-3 (cm)	[P] (mg/g)	[S] (%)	[Fe] (%)	[Cu] (µg/g)	[Cd] (µg/g)	[Pb] (µg/g)	[Ba] (µg/g)	[Zn] (µg/g)
1	2.96	0.46	6.11	37.44	11.80	46.26	206.34	172.43
2	3.31	0.48	6.69	59.89	13.09	48.67	240.87	202.05
3	3.12	0.44	9.60	62.90	13.25	44.52	276.24	211.08
4	2.73	0.49	5.52	58.31	12.25	45.69	238.06	181.34
5	2.34	0.57	7.06	43.92	12.33	45.68	214.15	186.34
6	2.34	0.28	7.26	31.49	13.02	41.61	158.55	166.52
7	2.68	0.38	6.07	36.35	13.45	51.38	212.73	235.11
8	2.47	0.44	5.51	40.95	12.01	36.02	202.35	159.78
9	2.28	0.46	6.44	39.77	10.78	36.47	208.15	150.94
10	2.18	0.47	6.91	50.05	12.89	46.82	275.16	177.56
11	2.14	0.47	4.74	31.38	10.45	42.90	213.13	135.78
12	2.47	0.60	5.85	38.52	11.68	37.27	254.07	174.81
13	2.57	0.52	7.20	43.01	12.95	46.31	270.92	196.07
14	2.20	0.84	7.69	66.90	12.81	48.71	255.15	187.92
15	2.07	0.44	14.25	22.02	11.10	33.96	209.56	145.83
16	2.25	0.60	6.39	25.83	12.15	39.85	240.46	174.84
17	2.42	0.43	6.68	23.46	11.51	40.10	230.89	154.85
18	3.04	0.56	6.47	29.32	13.01	46.45	255.61	211.75
19	2.76	0.69	5.94	25.36	12.40	46.63	202.96	190.29
20	2.39	0.41	8.31	24.66	11.58	40.73	221.60	180.32
21	2.49	0.41	7.39	16.96	12.45	46.60	246.04	204.61
22	1.92	0.41	5.42	23.52	12.37	43.81	243.02	195.70
23	2.61	0.22	5.61	18.35	10.47	29.29	171.79	105.07
24	3.28	0.53	8.27	14.81	11.36	46.81	198.89	182.06
25	2.69	0.35	6.26	28.08	13.42	47.80	272.82	225.63
26	2.21	0.26	5.82	21.32	10.95	38.48	224.17	170.39
27	2.73	0.35	6.24	25.06	11.80	47.21	234.37	171.63
28	2.63	0.42	5.27	19.62	12.42	51.79	228.85	197.32
29	2.43	0.35	7.37	22.79	11.74	46.34	235.19	170.10
31	2.60	0.39	6.58	18.17	11.83	52.73	228.40	184.90
32	2.36	0.41	3.91	27.60	11.51	47.04	239.28	175.92
33	2.05	0.56	6.43	25.77	11.37	42.58	205.30	168.18
34	2.64	0.52	6.07	26.33	12.15	49.07	268.08	168.94
35	2.17	0.39	7.75	20.77	10.12	38.36	204.60	179.00
36	2.40	0.27	0.11	19.55	13.04	59.53	254.33	210.70
37	2.35	0.36	0.19	20.46	12.25	56.97	233.22	192.36
38	2.32	0.23	7.10	22.04	12.45	59.80	239.86	201.01
39	2.31	0.27	8.90	24.35	11.77	51.13	228.09	190.31
40	2.29	0.35	7.39	23.62	12.18	53.40	217.42	192.65
41	1.98	0.36	6.62	24.36	12.03	56.79	235.20	179.80
43	2.79	0.37	5.39	23.70	13.72	65.91	224.33	194.43
44	2.05	0.28	7.50	22.35	12.15	63.42	232.01	210.28
45	2.12	0.24	8.07	20.19	11.20	46.34	190.02	172.77
46	2.70	0.31	6.56	17.28	12.58	58.84	217.70	216.78

ECS-3 (cm)	[P] (mg/g)	[S] (%)	[Fe] (%)	[Cu] (µg/g)	[Cd] (µg/g)	[Pb] (µg/g)	[Ba] (µg/g)	[Zn] (µg/g)
47	2.35	0.41	7.24	25.02	13.62	68.00	249.42	248.37
48	2.20	0.20	5.31	16.42	11.20	47.57	193.69	182.91
49	2.47	0.24	7.25	20.40	12.41	54.24	221.58	210.60
50	2.07	0.23	7.86	16.93	11.96	58.65	218.95	228.14
51	2.02	0.22	6.67	22.33	10.89	46.13	207.72	159.49
52	2.27	0.21	5.61	24.08	12.59	57.87	243.38	218.94
53	2.84	0.22	4.52	13.67	12.55	58.13	184.43	214.35
54	2.62	0.43	6.94	21.09	12.51	56.96	207.75	198.13
55	2.60	0.31	6.37	20.87	13.18	69.61	250.01	201.98
56	2.45	0.39	7.90	15.03	11.58	55.40	222.83	193.21
57	2.52	0.38	2.62	18.94	11.56	53.70	194.40	198.78
58	2.42	0.77	8.34	26.89	13.20	65.36	244.99	219.09
59	2.11	0.46	6.90	17.76	12.18	56.46	201.69	188.90
60	1.54	0.24	6.83	23.96	10.81	36.87	146.47	152.95
61	1.41	0.21	4.28	14.19	9.62	29.01	90.65	110.14
62	1.53	0.20	3.61	16.75	10.08	33.55	107.61	123.80
63	1.63	0.18	5.96	12.59	11.38	41.40	150.36	180.71
64	1.47	0.16	6.09	9.53	11.60	7.29	3.64	97.39
65	1.39	0.36	5.14	24.19	11.65	41.68	177.77	158.64
66	1.36	0.27	9.18	48.69	12.05	35.79	102.58	186.77
67	1.27	0.28	8.85	55.83	12.61	38.82	83.56	218.06
68	1.15	0.28	5.43	46.73	11.80	38.39	74.84	191.18
69	1.14	0.27	6.19	60.91	12.23	35.61	87.77	201.93
70	1.15	0.29	5.99	46.80	11.73	34.37	77.62	182.73
71	1.24	0.26	6.22	51.39	12.38	35.44	88.46	196.38
72	1.28	0.28	7.78	58.09	12.53	43.26	95.89	231.20
73	1.35	0.28	7.37	53.52	12.19	38.21	107.20	220.06
74	1.33	0.34	7.87	59.73	13.65	43.70	116.02	277.69
75	1.02	0.27	7.18	63.53	11.76	38.75	96.15	193.92
76	1.02	0.24	6.67	54.69	10.97	32.36	84.27	165.00
77	1.01	0.25	6.02	36.17	10.14	32.86	67.89	163.46
78	0.85	0.28	5.13	50.02	11.34	33.61	91.85	180.00
79	0.87	0.23	2.96	38.52	9.81	19.97	54.31	101.84
80	1.08	0.32	4.76	36.18	10.65	27.05	53.79	153.63
81	1.03	0.37	6.07	48.38	10.80	26.47	66.36	150.85
82	0.89	0.28	3.91	40.00	9.81	21.22	54.41	132.13
83	1.09	0.23	4.35	38.19	10.09	27.91	60.62	128.85
84	1.09	0.31	6.62	47.34	11.62	33.95	81.06	192.46
85	0.96	0.27	6.57	51.42	11.90	30.38	81.90	171.52
86	0.97	0.25	4.94	43.58	10.67	29.70	63.67	143.15
87	0.90	0.23	4.91	39.79	10.33	26.45	57.96	131.29
88	1.02	0.20	3.05	32.88	9.62	19.11	50.54	95.29
89	1.12	0.23	5.35	36.75	9.44	27.47	57.92	139.04
90	1.25	0.30	3.25	36.28	10.63	24.06	61.63	157.55
91	1.27	0.28	5.96	56.83	12.47	40.07	114.12	224.94
92	1.19	0.28	5.63	48.11	11.74	36.31	101.04	193.97

ECS-3 (cm)	[P] (mg/g)	[S] (%)	[Fe] (%)	[Cu] (µg/g)	[Cd] (µg/g)	[Pb] (µg/g)	[Ba] (µg/g)	[Zn] (µg/g)
93	1.13	0.26	4.86	48.50	11.37	32.34	87.38	181.73
94	1.09	0.25	4.11	51.08	11.29	36.23	93.91	178.09
95	0.91	0.22	5.40	32.56	10.11	31.45	69.73	143.01
96	0.87	0.20	5.91	36.51	9.73	24.87	57.86	117.49
97	0.95	0.21	4.94	46.62	10.79	27.76	78.58	148.86
98	0.91	0.18	5.49	33.90	9.45	25.29	72.43	117.01
99	0.87	0.22	3.42	40.59	10.24	26.49	61.52	124.28
100	0.80	0.14	2.88	22.48	8.21	18.41	36.68	75.63
101	1.00	0.18	3.81	23.50	9.15	23.04	46.00	96.45
102	0.96	0.22	3.22	35.03	9.92	20.95	51.91	124.36
103	0.92	0.16	4.38	24.18	9.10	22.06	48.15	93.30
104	0.86	0.19	3.79	38.67	9.78	20.22	51.60	119.62
105	0.85	0.18	2.57	28.89	10.05	16.47	39.31	80.08
106	0.85	0.19	2.20	28.80	9.41	14.63	37.96	84.84
107	0.65	0.14	2.56	19.43	7.65	16.90	36.70	76.71
108	0.90	0.15	4.13	30.74	8.74	15.49	55.86	88.08
109	0.67	0.28	6.19	48.82	11.76	37.12	89.69	190.80

ECS-1 Depth (cm)	Oxide (Fe-P) (mg/g)	Fe-P AR (mt/yr)	Authigenic (A-P) (mg/g)	Detrital (D-P) (mg/g)	Organic (O-P) (mg/g)	O-P AR (mt/yr)	Total reactive P (mg/g)
1	0.963	41.02	0.090	0.047	0.287	12.21	1.386
2	0.769	43.89	0.109	0.048	0.279	15.93	1.205
3	0.937	54.27	0.123	0.050	0.280	16.22	1.389
4	0.833	48.29	0.110	0.049	0.253	14.68	1.245
5	0.882	43.14	0.117	0.114	0.272	13.33	1.386
6	0.714	23.56	0.109	0.049	0.275	9.08	1.147
7	0.900	32.26	0.090	0.042	0.222	7.97	1.254
8	0.686	23.85	0.105	0.123	0.249	8.67	1.162
9	0.741	29.05	0.103	0.048	0.258	10.10	1.150
10	0.770	28.48	0.096	0.048	0.247	9.15	1.161
11	0.907	35.53	0.100	0.055	0.265	10.38	1.327
12	0.718	33.45	0.111	0.048	0.255	11.86	1.132
13	1.009	36.11	0.111	0.122	0.255	9.12	1.498
14	1.010	40.40	0.108	0.052	0.263	10.53	1.434
15	1.015	36.41	0.113	0.047	0.276	9.89	1.451
16	0.930	43.88	0.101	0.050	0.248	11.70	1.330
17	0.501	20.70	0.050	0.071	0.196	8.09	0.817
18	0.505	20.10	0.048	0.026	0.194	7.73	0.774
19	0.508	20.64	0.042	0.031	0.190	7.74	0.771
20	0.551	23.77	0.030	0.026	0.197	8.51	0.804
21	0.645	28.74	0.062	0.034	0.188	8.38	0.929
22	0.635	26.44	0.046	0.036	0.167	6.97	0.884
23	0.661	30.24	0.054	0.079	0.196	8.96	0.989
24	0.499	19.51	0.048	0.032	0.187	7.32	0.767
25	0.576	24.45	0.065	0.028	0.184	7.82	0.853
26	0.599	24.74	0.054	0.030	0.190	7.87	0.874
27	0.787	36.13	0.360	0.052	0.225	10.33	1.423
28	0.937	41.25	0.116	0.057	0.222	9.77	1.333
29	1.098	53.43	0.106	0.050	0.231	11.23	1.485
30	0.982	44.92	0.107	0.121	0.247	11.31	1.457
31	1.024	47.95	0.095	0.054	0.261	12.23	1.433
32	0.987	38.42	0.095	0.053	0.258	10.06	1.395
33	0.999	45.79	0.089	0.050	0.248	11.38	1.387
34	0.935	43.49	0.096	0.044	0.232	10.80	1.307
35	0.848	32.19	0.112	0.052	0.257	9.76	1.270
36	1.005	43.87	0.096	0.052	0.262	11.42	1.415
37	0.849	41.18	0.106	0.121	0.271	13.13	1.346
38	0.766	34.41	0.093	0.055	0.249	11.17	1.162

ECS-3 Depth (cm)	Oxide (Fe-P) (mg/g)	Fe-P AR (mt/yr)	Authigenic (A-P) (mg/g)	Detrital (D-P) (mg/g)	Organic (O-P) (mg/g)	O-P AR (mt/yr)	Total reactive P (mg/g)
1	1.414	30.40	0.122	0.045	0.322	10.40	1.903
2	1.569	31.13	0.128	0.048	0.341	12.46	2.085
3	1.796	31.57	0.133	0.047	0.356	11.39	2.331
4	1.424	32.36	0.138	0.048	0.357	11.01	1.966
5	1.365	32.77	0.122	0.050	0.337	10.58	1.874
6	1.163	34.71	0.116	0.048	0.340	13.04	1.668
7	1.159	35.58	0.104	0.045	0.311	12.42	1.619
8	1.301	35.74	0.116	0.052	0.292	10.98	1.761
9	1.542	36.48	0.123	0.038	0.288	13.31	1.991
10	1.329	37.43	0.099	0.048	0.276	12.00	1.753
11	1.328	37.93	0.104	0.041	0.268	12.40	1.742
12	1.452	39.11	0.118	0.041	0.293	12.56	1.905
13	1.427	40.63	0.128	0.051	0.291	12.81	1.897
14	1.019	40.68	0.110	0.048	0.292	14.77	1.469
15	1.277	40.88	0.114	0.051	0.295	12.23	1.737
16	1.167	41.25	0.102	0.054	0.300	12.96	1.622
17	1.228	41.55	0.117	0.047	0.307	12.55	1.699
18	1.303	42.72	0.121	0.050	0.297	13.75	1.771
19	1.603	42.75	0.124	0.051	0.293	11.86	2.070
20	1.273	43.51	0.105	0.048	0.311	16.37	1.737
21	1.226	44.02	0.127	0.054	0.336	15.97	1.743
22	1.457	44.51	0.124	0.094	0.309	13.46	1.983
23	1.374	45.04	0.138	0.053	0.312	17.90	1.876
24	1.645	45.30	0.125	0.053	0.278	14.40	2.100
25	1.604	45.99	0.112	0.058	0.293	16.94	2.067
26	1.409	47.46	0.114	0.054	0.253	13.40	1.829
27	1.004	50.47	0.125	0.053	0.303	16.15	1.485
28	1.466	51.50	0.107	0.052	0.306	15.58	1.932
29	1.012	52.33	0.119	0.058	0.290	15.84	1.480
30	1.528	52.91	0.122	0.030	0.302	16.18	1.982
31	1.272	52.95	0.113	0.048	0.294	17.63	1.727
32	1.460	54.04	0.112	0.062	0.294	14.88	1.927
33	1.250	55.50	0.108	0.054	0.281	13.18	1.693
34	1.228	55.75	0.112	0.049	0.262	15.52	1.652
35	1.142	58.00	0.102	0.058	0.301	15.92	1.604
36	1.109	60.43	0.110	0.048	0.235	13.56	1.503
37	1.324	60.43	0.111	0.049	0.277	16.40	1.761
38	1.425	79.14	0.129	0.053	0.307	18.39	1.914

ECS-1 Depth (cm)	[Fe] (wt%)	[Mn] (µg/g)
1	1.53	828.06
2	1.56	760.85
3	1.66	824.01
4	1.60	836.88
5	1.37	752.84
6	1.49	751.55
7	1.52	790.92
8	1.21	615.82
9	1.39	747.50
10	1.39	723.52
11	1.46	768.85
12	1.38	700.20
13	1.68	823.70
14	1.51	789.42
15	1.77	856.62
16	1.53	826.45
17	1.12	757.68
18	1.09	610.28
19	1.06	787.91
20	1.15	1158.84
21	1.36	984.51
22	1.23	887.26
23	1.31	988.20
24	1.05	565.81
25	1.16	598.12
26	1.31	1238.50
27	1.34	642.69
28	1.67	768.59
29	1.64	836.13
30	1.67	783.74
31	1.78	842.32
32	1.70	816.65
33	1.60	809.14
34	1.64	811.99
35	1.61	727.87
36	1.65	817.27
37	1.63	753.98
38	1.64	800.53

ECS-3 Depth (cm)	[Fe] (wt%)	[Mn] (µg/g)
1	1.04	1165.75
2	1.13	1145.54
3	1.21	1232.00
4	1.10	1016.73
5	1.14	1006.26
6	1.03	973.51
7	1.01	1042.04
8	1.01	1095.58
9	1.07	1211.14
10	0.95	1062.78
11	0.99	1135.66
12	0.99	1265.02
13	1.12	1188.23
14	1.05	910.62
15	1.12	1105.59
16	1.04	966.59
17	1.03	1029.25
18	1.00	1010.29
19	1.22	1161.96
20	1.06	985.42
21	1.10	1073.75
22	1.28	1161.32
23	1.11	1147.05
24	1.11	1119.72
25	1.08	1087.72
26	1.08	1106.59
27	0.78	806.51
28	1.21	1247.92
29	0.93	930.65
30	1.18	1160.73
31	1.12	1144.11
32	0.98	1043.83
33	1.15	1195.25
34	1.09	1039.25
35	0.98	1021.46
36	0.94	972.45
37	1.10	1095.24
38	1.01	1135.21

References

Brezonik, P.L., and Pollman, C.D., 1997, Phosphorus chemistry and cycling in Florida lakes: global issues and local perspectives, in Reddy, K.R., and others eds., Phosphorus geochemistry in subtropical ecosystems: Boca Raton, Lewis, p. 69-110.

Boström, B., Anderson, J.M., Fleisher, S., and Jansson, M., 1988, Exchange of phosphorus across the sediment-water interface, Hydrobiologia, 170, p. 229-244.

Campbell, P., and Torgerson, T., 1980, Maintenance of Iron Meromixis by Iron Redeposition in a Rapidly Flushed Monimolimnion, Can. J. Fish. Aquati. Sci. 37, p. 1303-1313.

Environmental Protection Agency, 2004, Contaminated Sediment Report to Congress, The incidence and severity of sediment contamination in surface waters of United States: National Sediment Quality Survey, 2nd ed. 280 p.

Flemming, C.A., and Trevors, J.T., 1989, Copper toxicity and chemistry in the environment: A review, Water, Air, and Soil Pollution, 44, p. 143-158.

Filippelli, G.M., Laidlaw, M., Raftis, R., and Latimer, J.C., 2005, Urban lead poisoning and medical geology: An unfinished story, GSA Today, v. 15, p. 4-11.

----------, Laidlaw, M., Atkins, R., and Latimer, J., 2000, Lead in surface soils of Marion County, Indiana. *GSA Abstracts with Programs*, 32 (4**)**: 13.

----------, and Delaney, M.L., 1996, Phosphorus geochemistry of equatorial Pacific sediments, Geochemica Cosmochimica Acta, 60, p. 1479-1495.

----------, and Souch, C., 1999, Effects of climate and landscape development on the terrestrial phosphorus cycle, Geology, 27(2), p. 171-174.

Gardner, W.S., and Eadie, B.J.,1980, Chemical factors controlling phosphorus cycling in lakes, In: Nutrient Cycling in the Great Lakes: A Summarization of Factors Regulating the Cycling of Phosphorus, Special Report No. 83, D. Scavia and R.A. Moll (eds.). Great Lakes Research Division, The University of Michigan, Ann Arbor, Michigan. p. 13-34.

Gray, H.H., 1989, Quaternary geologic map of Indiana: Bloomiongton, IN, Indiana Geological Survey Miscellaneous Map 49, scale 1:500,000.

Gray, H.H., Ault, C.H., and Keller, S.J., 1987, Bedrock geologic map of Indiana: Bloomington, IN, Indiana Geological Survey, Miscellaneous Map, 48, scale 1:500,000.

Green, W. R., 1996, Eutrophication trends inferred from hypolimnetic dissolved-oxygen dynamics within selected White River Reservoirs, Northern Arkansas-Southern Missouri, 1974-94: U.S. Geological Survey Water-Resources Investigations Report 96-4096, 52 p.

Hall, R. D., 1999, Geology of Indiana, 2nd Ed., IUPUI Department of Geology and the Center for Earth and Environmental Science, 153 p.

Hanesch, M., and Scholger, R., 2005, The influence of soil type on the magnetic susceptibility measured throughout soil profiles, Geophysical Journal International, 161, p. 50-56.

Herring, W.C., 1976, Technical atlas of the ground-water resources of Marion County, Indiana: State of Indiana, Department of Natural Resources, Division of Water, 53 p.
Holz, J.C., Hoagland, K.D., Spawn, R.L., Popp, A., and Andersen, J.L., 1997, Phytoplankton community response to reservoir aging, 1968-92, Hydrobiologia, 346, p. 183-192.
Hutchinson, G.E., 1975, A Treatise on Limnology, Vol. 1, Pt. 2, Chemistry of Lakes, JohnWiley and Sons, New York, 1013 p.
Indy Parks and Recreation, Eagle Creek Park, 2005, www.indygov.org, [Accessed 16 November 2005].
Juracek, K.E., 1997, Analysis of bottom sediment to estimate nonpoint-source phosphorus loads for 1981-96 in Hillsdale Lake, Northeast Kansas: U.S. Geological Survey Water-Resources Investigations Report 97-4235, 26 p.
Kuwabar, J.S., Berelson, W.M., Balistrieri, L.S., Woods, P.F., Topping, B.R., Douglas, J.S., and Krabbenhoft, D.P., 2000, Benthic flux of metals and nutrients into the water column of Lake Coeur d'Alene, Idaho: Report of an August, 1999, pilot study: U.S. Geological Survey Water-Resources Investigations Report 00-4132, 62 p.
National Resource Conservation Service (NRCS), 2004, Marion County Soil Data, http://ssldata.nrcs.usda.gov.
Normandin, R.F., 1975, Copper Sulfate: Its use as an algaecide, New England Interstate Water Pollution Control Commission Boston, Massachusetts, 34 p.
Laenen, A., and LeTourneau, A.P., 1996, Upper Klamath Basin nutrient-loading study estimate of wind-induced resuspension of bed sediment during periods of low lake elevation: U.S. Geological Survey Open-File Report, 11 p.
Larsen, D.P., Schults, D.W., and Malueg, K.W., 1981, Summer Internal Phosphorus Supplies in Shagawa Lake, Minnesota, Limnology and Oceanography, 26(4), p. 740-753.
Lwanga, M.S., Kansiime, F., Denny, P., Scullion, J., 2003, Heavy metals in Lake George, Uganda, with relation to metal concentrations in tissues of common fish species, Hydrobiolgia, 499, 83-93.
Milligan, C.R. and Pope, L.M., 2001, Occurrence of phosphorus, nitrate, and suspended solids in streams of the Chaney Reservoir Watershed, South-Central Kansas, 1997-2000: U.S. Geological Survey Water-Resources Investigations Report 01 4199, 18 p.
Moore, J.N., and Luoma, S.N., 1990, Hazardous wastes from large-scale metal extraction, Environ. Sci. Technolo., 24, p. 1278-1285.
Morris, G.L., and Fan, J., 1998, Reservoir sedimentation handbook design and management of dams, reservoirs, and watersheds for sustainable use: New York, McGraw Hill.
Mortimer, C.H., 1941, The exchange of dissolved substances between mud and water in lakes, The Journal of Ecology, 29(2), p. 280-329.
----------, 1942, The exchange of dissolved substances between mud and water in lakes, The Journal of Ecology, 30(1), p. 147-201.

----------, 1971, Chemical exchanges between sediments and water in the Great Lakes-speculations on probable regulatory mechanisms, Limnology and Oceanography, 16(2), p. 387-404.
National Weather Service, 1997, Historical climate summaries for Indiana: Internet Universal Locator http://www.nws.noaa.gov.
Normandin, R. F., 1975, Copper sulfate: Its use as an algaecide based on a history of its use in a New Hampshire waters 1960-1975, Boston, N.E. Interstate Water Pollution Control Commision, 34 p.
Nowacki, J., 2003, Personal communication.
Nürnberg, G.K., 1984, The prediction of internal phosphorus load in lakes with anoxic hypolimnia, Limnology and Oceanography, 29(1), p. 111-124.
----------, 1985, Availability of phosphorus upwelling from iron-rich anoxic hypolimnia, Arch. Hydrobiol., 104(4) p. 459-476.
----------, 1987, A comparison of internal phosphorus loads in lakes with anoxic hypolimnia: Laboratory incubation versus in situ hypolimnetic phosphorus accumulation, Limnology and Oceanography, 32(5), p. 1160-1164.
----------, 1995, Quantifying anoxia in lakes, Limnology and Oceanography, 40(6), p.1100-1111.
Perkins, S., 2000, Airborne trace metal contamination of wetland sediments at Indiana Dunes National Lakeshore, Air, Water, and Soil Pollution, 122(1-2), p. 231-260.
Roden, E.E., and Edmonds, J.W., 1997, Phosphate mobilization in iron-rich anaerobic sediments: microbial Fe(III) reduction versus iron-sulfide formation, Arch. Hydrobiol., 139(3), p. 347-378.
Ruttenberg, K.C., 1992, Development of a sequential extraction method for different forms of phosphorus in marine sediments, Limnology and Oceanography, 27(7), p. 1460-1482.
Schlesinger, W.H., 1997, Biogeochemistry an analysis of global change: San Diego, Academic Press, 588 p.
Schneider, A.F., 1966, Physiography, in Lindsey, A.A., ed., Natural features of Indiana: Indianapolis, Indiana Academy of Science, p. 45-56.
Schnoebelen, D.J., Fenelon, J.M., Baker, N.T., Martin, J.D., Bayless, E.R., Jacques, D.V., and Crawford, C.G., 1999, Environmental setting and natural factors and human influences affecting water quality in the White River basin, Indiana: U.S. Geological Survey Water Resources Investigations Report 97-4206, 66 p.
Sharpley, A.N., 1997, Global issues of phosphorus in terrestrial ecosystems, in Reddy, K.R., and others eds., Phosphorus geochemistry in subtropical ecosystems: Boca Raton, Lewis, p. 15-46.
Soil Survey Staff, Natural Resources Conservation Service, United States Department of Agriculture, Soil Series Classification Database, Available URL: http://soils.usda.gov/soils/technical/classification/scfile/index.html,[Accessed 16 November 2005].
Song, Y., and Muller, G., 1999, Sediment-water interactions in anoxic freshwater sediments, mobility of heavy metals and nutrients, Berlin, Springer, 111 p.

Spencer, D.F., 1981, Limnological analysis of Eagle Creek Reservoir: characterization of chemical and biological components and a preliminary total phosphorus budget, in: The Holcomb Research Institute and the Indiana Heartland Model Implementation Project, R.F. Hyde, I.A. Goldblatt, and B.J. Stolz., eds.

Strøm, K.M., 1933, Nutrition of algae, experiments upon: The feasibility of the Schrieber Method in fresh waters; the relative importance of iron and manganese in the nutritive medium; the nutritive substance given off by lake bottom muds, Arch. Hydrobiol. 25, p. 38-47.

Tedesco, L.P., Atekwana, E.A., Filippelli, G.M., Licht, K., Shrake, L., Hall, B.E., Pascual, D.L., Latimer, J., Raftis, R., Sapp, D., Lindsey, G., Maness, R., Pershing, D., Peterson, D., Ozekin, K., Mysore, C., and Prevost, M., 2003, Water quality and nutrient cycling in three Indiana watersheds and their reservoirs: Eagle Creek/Eagle Creek Reservoir, Fall Creek/Geist Reservoir, and Cicero Creek/Morse Reservoir, Central Indiana Water Resources Partnership, CEES Publication 2003-01, IUPUI, Indianapolis, IN, 163 p.

Thienemann, A., 1928, The oxygen in an eutrophic and oligotrophic lake, a contribution to sea-typology, Die Binnengwässer 4, 175 p.

U.S. Geological Survey, 1990, Land use and land cover digital data from 1:125,000- and 1:100,000-scale maps, Data users guide 4: Reston, Va., U.S. Geological Survey, 25 p.

Vollenweider, R.A., 1968, Scientific fundamentals of the eutrophication of lakes and flowing waters, with particular reference to nitrogen and phosphorus, Organization for economic cooperation and development (OECD) report DAS/CSI/68.27, Paris, 192 p.

Wangsness, D.J., 1983, Water and streambed-material data, Eagle Creek Watershed, Indiana August 1980, October and December 1982, and April 1983; Updating of U.S. Geological Survey Open-File Report 83-215, Open File Report 83-532, USGS, 51 p.

Wetzel, Robert G., 2001, Limnology (3d ed): Orlando, Harcourt Brace Jovanovich, 1006 p.

CURRICULUM VITAE

Robyn R. Raftis

EDUCATION

M.S.: Environmental Geology, Indiana University at Indianapolis (IUPUI), 2007.
Thesis: *Internal Cycling in an Urban Drinking Water Reservoir*.

B.A.: Geology, Indiana University at Indianapolis (IUPUI), 2000.
Thesis: *A comparison of Lead Concentrations in Soils along two roadways in Marion County, Indianapolis, Indiana.*

PROFESSIONAL EXPERIENCE

Geologist, Indiana Department of Environmental Management. 2007. Responsible for evaluation of site characterization and environmental remediation work conducted in Indiana.

Geologist, Environmental Services Associates, LLC. 2005-2006. Performed soil boring analysis and environmental assessment services.

Teaching Assistant, IUPUI Geology. 2003. Responsible for preparation and teaching of introductory environmental geology lecture.

Research Assistant, IUPUI Geochemistry Laboratory. 1997-2002. Performed sediment processing and analysis, including utilization of ICP-AES, Microwave Digestion System, Mercury Analyzer, and Coulometer.

Research Assistant, IUPUI Sediment Analysis Laboratory. 2002. Performed sediment processing and analysis, including microscope work and use of the Malvern particle size analyzer.

AWARDS AND GRANTS

IUPUI Graduate Student Organization Educational Enhancement Grant, 2003
Indiana University Graduate School Travel Fellowship, 2003
Geological Society of America Grant, 2002
IUPUI Geology Outstanding Academic Achievement, 2001
IUPUI Undergraduate Research Opportunity Program Grant, 1999
Undergraduate Research Symposium Award, 2000

PUBLISHED ABSTRACTS

Filippelli, G., Laidlaw, M., Mielke, H., Johnson, D., Gonzalez, C., Latimer, J., and Raftis, R. 2005. Developing Predictive Tools for Optimizing Health Care Using Medical Geology: An Example from Urban Lead Poisoning. GSA Abstracts with Programs. 37(7):178-179.

Raftis, R., Pascual, D. L., Filippelli, G., Tedesco, L., and Gray, M. 2005. Phosphorus Mass Balance of an Eutrophied Drinking Water Reservoir; Eagle Creek Reservoir, Indianapolis, Indiana. GSA Abstracts with Programs. 37(7):353.

Raftis, R., Filippelli, G., Tedesco, L., Atekwana, E., Souch, C., Latimer, J., Pascual, D.L., and Shrake, L. 2003. Nutrient Cycling and Water Quality in an Urban Drinking Water Reservoir. GSA Abstracts with Programs. 35(6):145.

Raftis, R., Filippelli, G., Tedesco, L., Atekwana, E., Licht, K., Souch, C., Latimer, J., Pascual, D., and Shrake, L. 2003. Internal Phosphorus Cycling in an Urban Drinking Water Reservoir. GSA Abstracts with Programs. 35(6):59.

Filippelli, G., Laidlaw, M., Latimer, J., and Raftis, R. 2002. Diffuse Lead and Children's Blood-Lead Levels in Indianapolis. GSA Abstracts with Programs. 34(6):146.

Filippelli, G., Latimer, J., Laidlaw, M., and Raftis, R. 2000. Lead In Surface Soils of Marion County, Indiana. GSA Abstracts with Programs. 32(5):30.

PUBLISHED ARTICLE

Filippelli, G., Laidlaw, M., Latimer, J., and Raftis, R. 2005. Urban Lead Poisoning and Medical Geology; An Unfinished Story. GSA Today 15(1):4-11.